

Unsupervised Reinforcement Learning in Multiple Environments

Mirco Mutti^{1,2,*}, Mattia Mancassola^{1,*}, and Marcello Restelli¹

¹ Politecnico di Milano, Milan, Italy

² Università di Bologna, Bologna, Italy

mirco.mutti@polimi.it, mattia.mancassola@mail.polimi.it, marcello.restelli@polimi.it

Abstract

Several recent works have been dedicated to unsupervised reinforcement learning in a single environment, in which a policy is first pre-trained with unsupervised interactions, and then fine-tuned towards the optimal policy for several downstream supervised tasks defined over the same environment. Along this line, we address the problem of unsupervised reinforcement learning in a class of multiple environments, in which the policy is pre-trained with interactions from the whole class, and then fine-tuned for several tasks in any environment of the class. Notably, the problem is inherently multi-objective as we can trade off the pre-training objective between environments in many ways. In this work, we foster an exploration strategy that is sensitive to the most adverse cases within the class. Hence, we cast the exploration problem as the maximization of the mean of a critical percentile of the state visitation entropy induced by the exploration strategy over the class of environments. Then, we present a policy gradient algorithm, α MEPOL, to optimize the introduced objective through mediated interactions with the class. Finally, we empirically demonstrate the ability of the algorithm in learning to explore challenging classes of continuous environments and we show that reinforcement learning greatly benefits from the pre-trained exploration strategy w.r.t. learning from scratch.

1 Introduction

The typical Reinforcement Learning (RL, Sutton and Barto 2018) setting involves a learning agent interacting with an environment in order to maximize a reward signal. In principle, the reward signal is a given and perfectly encodes the task. In practice, the reward is usually hand-crafted, and designing it to make the agent learn a desirable behavior is often a huge challenge. This poses a serious roadblock on the way of autonomous learning, as any task requires a costly and specific formulation, while the synergy between solving one RL problem and another is very limited. To address this crucial limitation, several recent works (Mutti, Pratissoli, and Restelli 2021; Liu and Abbeel 2021b,a; Seo et al. 2021; Yarats et al. 2021) have been dedicated to *unsupervised* RL. In this framework, originally envisioned in (Hazan et al. 2019; Mutti and Restelli 2020), the agent first pre-trains its policy by taking a

large amount of unsupervised interactions with the environment (*unsupervised pre-training*). Then, the pre-trained policy is transferred to several downstream tasks, each of them defined through a reward function, and the agent has to learn an optimal policy by taking additional supervised interactions with the environment (*supervised fine-tuning*). Whereas most of the existing works in unsupervised RL (Campos et al. (2021) make for a notable exception) converged to a straightforward fine-tuning strategy, in which the pre-trained policy is employed as an exploratory initialization of a standard RL algorithm, there is lesser consensus on which unsupervised objective is best suited for the pre-training phase. Traditional intrinsic motivation bonuses that were originally designed to address exploration in supervised RL (e.g., Pathak et al. 2017; Burda et al. 2019) can be employed in the unsupervised RL setting as well (Laskin et al. 2021). However, these bonuses are designed to vanish over time, which makes it hard to converge to a stable policy during the unsupervised pre-training. The *Maximum State Visitation Entropy* (MSVE, Hazan et al. 2019) objective, which incentivizes the agent to learn a policy that maximizes the entropy of the induced state visitation, emerged as a powerful alternative in both continuous control and visual domains (Laskin et al. 2021). The intuition underlying the MSVE objective is that a pre-trained exploration strategy should visit with high probability any state where the agent might be rewarded in a subsequent supervised task, so that the fine-tuning to the optimal policy is feasible. Although unsupervised pre-training methods effectively reduce the reliance on a reward function and lead to remarkable fine-tuning performances w.r.t. RL from scratch, all of the previous solutions to unsupervised RL assume the existence of a single environment.

In this work, we aim to push the generality of this framework even further, by addressing the problem of *unsupervised RL in multiple environments*. In this setting, during the pre-training the agent faces a class of reward-free environments that belong to the same domain but differ in their transition dynamics. At each turn of the learning process, the agent is drawn into an environment within the class, where it can interact for a finite number of steps before facing another turn. The ultimate goal of the agent is to pre-train an exploration strategy that helps to solve *any* subsequent fine-tuning task that can be specified over *any* environment of the class.

Our contribution to the problem of unsupervised RL in

*These authors contributed equally. The implementation of α MEPOL is available at <https://github.com/muttimiro/alphamepol>. Copyright © 2022, Association for the Advancement of Artificial Intelligence (www.aaai.org). All rights reserved.

multiple environments is three-fold: First, we frame the problem into a tractable *formulation* (Section 4), then, we propose a *methodology* to address it (Section 5), for which we provide a thorough *empirical* evaluation (Section 6). Specifically, we extend the pre-training objective to the multiple-environments setting. Notably, when dealing with multiple environments the pre-training becomes a *multi-objective* problem, as one could establish any combination of preferences over the environments. Previous unsupervised RL methods would blindly optimize the average of the pre-training objective across the class, implicitly establishing a uniform preference. Instead, in this work we consider the mean of a critical percentile of the objective function, i.e., its Conditional Value-at-Risk (CVaR, Rockafellar, Uryasev et al. 2000) at level α , to prioritize the performance in particularly rare or adverse environments. In line with the MSVE literature, we chose the CVaR of the induced state visitation entropy as the pre-training objective, and we propose a policy gradient algorithm (Deisenroth, Neumann, and Peters 2013), α -sensitive *Maximum Entropy POLicy optimization* (α MEPOL), to optimize it via mere interactions with the class of environments. As in recent works (Mutti, Pratissoli, and Restelli 2021; Liu and Abbeel 2021b; Seo et al. 2021), the algorithm employs non-parametric methods to deal with state entropy estimation in continuous and high-dimensional environments. Then, it leverages these estimated values to optimize the CVaR of the entropy by following its policy gradient (Tamar, Glassner, and Mannor 2015). Finally, we provide an extensive experimental analysis of the proposed method in both the unsupervised pre-training over classes of multiple environments, and the supervised fine-tuning over several tasks defined over the class. The exploration policy pre-trained with α MEPOL allows to solve sparse-rewards tasks that are impractical to learn from scratch, while consistently improving the performance of a pre-training that is blind to the unfavorable cases.

2 Related Work

In this section, we revise the works that relates the most with the setting of unsupervised RL in multiple environments. A more comprehensive discussion can be found in Appendix A.

In a previous work, Rajendran et al. (2020) considered a learning process composed of agnostic pre-training (called a *practice*) and supervised fine-tuning (a *match*) in a class of environments. However, in their setting the two phases are alternated, and the supervision signal of the matches allows to learn the reward for the practice through a meta-gradient.

Parisi et al. (2021) addresses the unsupervised RL in multiple environments concurrently to our work. Whereas their setting is akin to ours, they come up with an essentially orthogonal solution. Especially, they consider a pre-training objective inspired by count-based methods (Bellemare et al. 2016) in place of our entropy objective. Whereas they design a specific bonus for the multiple-environments setting, they essentially establish a uniform preference over the class instead of prioritizing the worst-case environment as we do.

Finally, our framework resembles the *meta-RL* setting (Finn, Abbeel, and Levine 2017), in which we would call *meta-training* the unsupervised pre-training, and *meta-testing* the supervised fine-tuning. However, none of the existing

works combine unsupervised meta-training (Gupta et al. 2018a) with a multiple-environments setting.

3 Preliminaries

A vector v is denoted in bold, and v_i stands for its i -th entry.

Probability and Percentiles Let X be a random variable distributed according to a cumulative density function (cdf) $F_X(x) = Pr(X \leq x)$. We denote with $\mathbb{E}[X]$, $\text{Var}[X]$ the expected value and the variance of X respectively. Let $\alpha \in (0, 1)$ be a confidence level, we call the α -percentile (shortened to $\alpha\%$) of the variable X its Value-at-Risk (VaR), which is defined as

$$\text{VaR}_\alpha(X) = \inf \{x \mid F_X(x) \geq \alpha\}.$$

Analogously, we call the mean of this same α -percentile the Conditional Value-at-Risk (CVaR) of X ,

$$\text{CVaR}_\alpha(X) = \mathbb{E}[X \mid X \leq \text{VaR}_\alpha(X)].$$

Markov Decision Processes A Controlled Markov Process (CMP) is a tuple $\mathcal{M} := (\mathcal{S}, \mathcal{A}, P, D)$, where \mathcal{S} is the state space, \mathcal{A} is the action space, the transition model $P(s'|a, s)$ denotes the conditional probability of reaching state s' when selecting action a in state s , and D is the initial state distribution. The behavior of an agent is described by a policy $\pi(a|s)$, which defines the probability of taking action a in s . Let Π be the set of all the policies. Executing a policy π in a CMP over T steps generates a trajectory $\tau = (s_{0,\tau}, a_{0,\tau}, \dots, a_{T-2,\tau}, s_{T-1,\tau})$ such that $p_{\pi, \mathcal{M}}(\tau) = D(s_{0,\tau}) \prod_{t=0}^{T-1} \pi(a_{t,\tau}|s_{t,\tau}) P(s_{t+1,\tau}|s_{t,\tau}, a_{t,\tau})$ denotes its probability. We denote the state-visitation frequencies induced by τ with $d_\tau(s) = \frac{1}{T} \sum_{t=0}^{T-1} \mathbb{1}(s_{t,\tau} = s)$, and we call $d_\pi^\mathcal{M} = \mathbb{E}_{\tau \sim p_{\pi, \mathcal{M}}}[d_\tau]$ the marginal state distribution. We define the differential entropy (Shannon 1948) of d_τ as $H(d_\tau) = -\int_{\mathcal{S}} d_\tau(s) \log d_\tau(s) ds$. For simplicity, we will write $H(d_\tau)$ as a random variable $H_\tau \sim \delta(h - H(d_\tau)) p_{\pi, \mathcal{M}}(\tau)$, where $\delta(h)$ is a Dirac delta.

By coupling a CMP \mathcal{M} with a reward function R we obtain a Markov Decision Process (MDP, Puterman 2014) $\mathcal{M}^R := \mathcal{M} \cup R$. Let $R(s, a)$ be the expected immediate reward when taking $a \in \mathcal{A}$ in $s \in \mathcal{S}$ and let $R(\tau) = \sum_{t=0}^{T-1} R(s_{t,\tau}, a_{t,\tau})$, the *performance* of a policy π over the MDP \mathcal{M}^R is defined as

$$\mathcal{J}_{\mathcal{M}^R}(\pi) = \mathbb{E}_{\tau \sim p_{\pi, \mathcal{M}}}[R(\tau)]. \quad (1)$$

The goal of reinforcement learning (Sutton and Barto 2018) is to find an optimal policy $\pi_\mathcal{J}^* \in \arg \max \mathcal{J}_{\mathcal{M}^R}(\pi)$ through sampled interactions with an unknown MDP \mathcal{M}^R .

4 Unsupervised RL in Multiple Environments

Let $\mathcal{M} = \{\mathcal{M}_1, \dots, \mathcal{M}_I\}$ be a class of unknown CMPs, in which every element $\mathcal{M}_i = (\mathcal{S}, \mathcal{A}, P_i, D)$ has a specific transition model P_i , while $\mathcal{S}, \mathcal{A}, D$ are homogeneous across the class. At each turn, the agent is able to interact with a single environment $\mathcal{M} \in \mathcal{M}$. The selection of the environment to interact with is mediated by a distribution $p_\mathcal{M}$ over \mathcal{M} ,

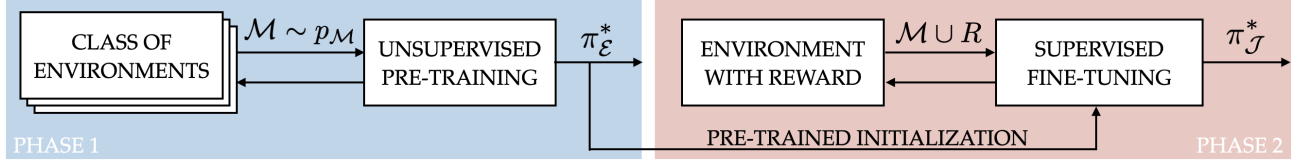


Figure 1: On the left, we highlight the unsupervised pre-training, in which the agent iteratively interacts with a CMP $\mathcal{M} \in \mathcal{M}$ drawn from $p_{\mathcal{M}}$. The pre-trained policy $\pi_{\mathcal{E}}^*$ conveys the initialization to the subsequent supervised fine-tuning (on the right), which outputs a reward maximizing policy $\pi_{\mathcal{J}}^*$ for an MDP $\mathcal{M} \cup R$ that pairs $\mathcal{M} \in \mathcal{M}$ with an arbitrary reward function R .

outside the control of the agent. The aim of the agent is to pre-train an exploration strategy that is general across all the MDPs \mathcal{M}^R one can build upon \mathcal{M} . In a single-environment setting, this problem has been assimilated to learning a policy that maximizes the entropy of the induced state visitation frequencies (Hazan et al. 2019; Mutti and Restelli 2020). One can straightforwardly extend the objective to multiple environments by considering the expectation over the class of CMPs, $\mathcal{E}_{\mathcal{M}}(\pi) = \mathbb{E}_{\mathcal{M} \sim p_{\mathcal{M}}} [H_{\tau}]$, where the usual entropy

objective over the single environment \mathcal{M}_i can be easily recovered by setting $p_{\mathcal{M}_i} = 1$. However, this objective function does not account for the tail behavior of H_{τ} , i.e., for the performance in environments of \mathcal{M} that are rare or particularly unfavorable. This is decidedly undesirable as the agent may be tasked with an MDP built upon one of these adverse environments in the subsequent supervised fine-tuning, where even an optimal strategy w.r.t. $\mathcal{E}_{\mathcal{M}}(\pi)$ may fail to provide sufficient exploration. To overcome this limitation, we look for a more nuanced exploration objective that balances the expected performance with the sensitivity to the tail behavior. By taking inspiration from the risk-averse optimization literature (Rockafellar, Uryasev et al. 2000), we consider the CVaR of the state visitation entropy induced by π over \mathcal{M} ,

$$\begin{aligned} \mathcal{E}_{\mathcal{M}}^{\alpha}(\pi) &= \text{CVaR}_{\alpha}(H_{\tau}) \\ &= \mathbb{E}_{\substack{\mathcal{M} \sim p_{\mathcal{M}} \\ \tau \sim p_{\pi, \mathcal{M}}}} [H_{\tau} \mid H_{\tau} \leq \text{VaR}_{\alpha}(H_{\tau})], \end{aligned} \quad (2)$$

where α is a confidence level and $\mathcal{E}_{\mathcal{M}}^1(\pi) := \mathcal{E}_{\mathcal{M}}(\pi)$. The lower we set the value of α , the more we hedge against the possibility of a bad exploration outcome in some $\mathcal{M} \in \mathcal{M}$. In the following sections, we propose a method to effectively learn a policy $\pi_{\mathcal{E}}^* \in \arg \max \mathcal{E}_{\mathcal{M}}^{\alpha}(\pi)$ through mere interactions with \mathcal{M} , and we show how this serves as a pre-training for RL (the full process is depicted in Figure 1). A preliminary theoretical characterization of the problem of optimizing $\mathcal{E}_{\mathcal{M}}^{\alpha}(\pi)$ is provided in Appendix B.

5 A Policy Gradient Approach

In this section, we present an algorithm, called *α -sensitive Maximum Entropy Policy optimization* (α MEPOL), to optimize the exploration objective in (2) through mediated interactions with a class of continuous environments.

α MEPOL operates as a typical policy gradient approach (Deisenroth, Neumann, and Peters 2013). It directly searches for an optimal policy by navigating a set of parametric differentiable policies $\Pi_{\Theta} := \{\pi_{\theta} : \theta \in \Theta \subseteq \mathbb{R}^n\}$. It does

so by repeatedly updating the parameters θ in the gradient direction, until a stationary point is reached. This update has the form

$$\theta' = \theta + \beta \nabla_{\theta} \mathcal{E}_{\mathcal{M}}^{\alpha}(\pi_{\theta}),$$

where β is a learning rate, and $\nabla_{\theta} \mathcal{E}_{\mathcal{M}}^{\alpha}(\pi_{\theta})$ is the gradient of (2) w.r.t. θ . The following proposition provides the formula of $\nabla_{\theta} \mathcal{E}_{\mathcal{M}}^{\alpha}(\pi_{\theta})$. The derivation follows closely the one in (Tamar, Glassner, and Mannor 2015, Proposition 1), which we have adapted to our objective function of interest (2).

Proposition 5.1. *The policy gradient of the exploration objective $\mathcal{E}_{\mathcal{M}}^{\alpha}(\pi_{\theta})$ w.r.t. θ is given by*

$$\begin{aligned} \nabla_{\theta} \mathcal{E}_{\mathcal{M}}^{\alpha}(\pi_{\theta}) &= \mathbb{E}_{\substack{\mathcal{M} \sim p_{\mathcal{M}} \\ \tau \sim p_{\pi_{\theta}, \mathcal{M}}}} \left[\left(\sum_{t=0}^{T-1} \nabla_{\theta} \log \pi_{\theta}(a_{t,\tau} | s_{t,\tau}) \right) \right. \\ &\quad \times \left. \left(H_{\tau} - \text{VaR}_{\alpha}(H_{\tau}) \right) \mathbb{1}_{H_{\tau} \leq \text{VaR}_{\alpha}(H_{\tau})} \right]. \end{aligned}$$

However, in this work we do not assume full knowledge of the class of CMPs \mathcal{M} , and the expected value in Proposition 5.1 cannot be computed without having access to $p_{\mathcal{M}}$ and $p_{\pi_{\theta}, \mathcal{M}}$. Instead, α MEPOL computes the policy update via a Monte Carlo estimation of $\nabla_{\theta} \mathcal{E}_{\mathcal{M}}^{\alpha}$ from the sampled interactions $\{(\mathcal{M}_i, \tau_i)\}_{i=1}^N$ with the class of environments \mathcal{M} . The policy gradient estimate itself relies on a Monte Carlo estimate of each entropy value H_{τ_i} from τ_i , and a Monte Carlo estimate of $\text{VaR}_{\alpha}(H_{\tau})$ given the estimated $\{H_{\tau_i}\}_{i=1}^N$. The following paragraphs describe how these estimates are carried out, while Algorithm 1 provides the pseudocode of α MEPOL. Additional details and implementation choices can be found in Appendix D.

Entropy Estimation We would like to compute the entropy H_{τ_i} of the state visitation frequencies d_{τ_i} from a single realization $\{s_{t,\tau_i}\}_{t=0}^{T-1} \subset \tau_i$. This estimation is notoriously challenging when the state space is continuous and high-dimensional $\mathcal{S} \subseteq \mathbb{R}^p$. Taking inspiration from recent works pursuing the MSVE objective (Mutti, Pratissoli, and Restelli 2021; Liu and Abbeel 2021b; Seo et al. 2021), we employ a principled k -Nearest Neighbors (k -NN) entropy estimator (Singh et al. 2003) of the form

$$\hat{H}_{\tau_i} \propto -\frac{1}{T} \sum_{t=0}^{T-1} \log \frac{k \Gamma(\frac{p}{2} + 1)}{T \|s_{t,\tau_i} - s_{t,\tau_i}^{k\text{-NN}}\|^p \pi^{\frac{p}{2}}}, \quad (3)$$

where Γ is the Gamma function, $\|\cdot\|$ is the Euclidean distance, and $s_{t,\tau_i}^{k\text{-NN}} \in \tau_i$ is the k -nearest neighbor of s_{t,τ_i} . The intuition behind the estimator in (3) is simple: We can suppose

Algorithm 1: α MEPOL

Input: percentile α , learning rate β **Output:** policy π_θ

```

1: initialize  $\theta$ 
2: for epoch = 0, 1, ..., until convergence do
3:   for  $i = 1, 2, \dots, N$  do
4:     sample an environment  $\mathcal{M}_i \sim p_{\mathcal{M}}$ 
5:     sample a trajectory  $\tau_i \sim p_{\pi_\theta, \mathcal{M}_i}$ 
6:     estimate  $H_{\tau_i}$  with (3)
7:   end for
8:   estimate  $\text{VaR}_\alpha(H_\tau)$  with (4)
9:   estimate  $\nabla_{\theta} \mathcal{E}_{\mathcal{M}}^\alpha(\pi_\theta)$  with (5)
10:  update parameters  $\theta \leftarrow \theta + \beta \widehat{\nabla}_{\theta} \mathcal{E}_{\mathcal{M}}^\alpha(\pi_\theta)$ 
11: end for

```

the state visitation frequencies d_{τ_i} to have a high entropy as long as the average distance between any encountered state and its k -NN is large. Despite its simplicity, a Euclidean metric suffices to get reliable entropy estimates in continuous control domains (Mutti, Pratissoli, and Restelli 2021).

VaR Estimation The last missing piece to get a Monte Carlo estimate of the policy gradient $\nabla_{\theta} \mathcal{E}_{\mathcal{M}}^\alpha$ is the value of $\text{VaR}_\alpha(H_\tau)$. Being $H_{[1]}, \dots, H_{[N]}$ the order statistics out of the estimated values $\{\hat{H}_{\tau_i}\}_{i=1}^N$, we can naïvely estimate the VaR as

$$\widehat{\text{VaR}}_\alpha(H_\tau) = H_{[\lceil \alpha N \rceil]}. \quad (4)$$

Albeit asymptotically unbiased, the VaR estimator in (4) is known to suffer from a large variance in finite sample regimes (Kolla et al. 2019), which is aggravated by the error in the upstream entropy estimates, which provide the order statistics. This variance is mostly harmless when we use the estimate to filter out entropy values beyond the $\alpha\%$, i.e., the condition $H_\tau \leq \text{VaR}_\alpha(H_\tau)$ in Proposition 5.1. Instead, its impact is significant when we subtract it from the values within the $\alpha\%$, i.e., the term $H_\tau - \text{VaR}_\alpha(H_\tau)$ in Proposition 5.1. To mitigate this issue, we consider a convenient baseline $b = -\text{VaR}_\alpha(H_\tau)$ to be subtracted from the latter, which gives the Monte Carlo policy gradient estimator

$$\widehat{\nabla}_{\theta} \mathcal{E}_{\mathcal{M}}^\alpha(\pi_\theta) = \sum_{i=1}^N f_{\tau_i} \hat{H}_{\tau_i} \mathbb{1}(\hat{H}_{\tau_i} \leq \widehat{\text{VaR}}_\alpha(H_\tau)), \quad (5)$$

where $f_{\tau_i} = \sum_{t=0}^{T-1} \nabla_{\theta} \log \pi_{\theta}(a_{t,\tau_i} | s_{t,\tau_i})$. Notably, the baseline b trades off a lower estimation error for a slight additional bias in the estimation (5). We found that this baseline leads to empirically good results and we provide some theoretical corroboration over its benefits in Appendix D.1.

6 Empirical Evaluation

We provide an extensive empirical evaluation of the proposed methodology over the two-phase learning process described in Figure 1, which is organized as follows:

- 6.1 We show the ability of our method in pre-training an exploration policy in a class of continuous gridworlds, emphasizing the importance of the percentile sensitivity;

- 6.2 We discuss how the choice of the percentile of interest affects the exploration strategy;
- 6.3 We highlight the benefit that the pre-trained strategy provides to the supervised fine-tuning on the same class;
- 6.4 We verify the scalability of our method with the size of the class, by considering a class of 10 continuous gridworlds;
- 6.5 We verify the scalability of our method with the dimensionality of the environments, by considering a class of 29D continuous control Ant domains;
- 6.6 We verify the scalability of our method with visual inputs, by considering a class of 147D MiniGrid domains;
- 6.7 We show that the pre-trained strategy outperforms a policy meta-trained with MAML (Finn, Abbeel, and Levine 2017; Gupta et al. 2018a) on the same class.

A thorough description of the experimental setting is provided in Appendix E.

6.1 Unsupervised Pre-Training with Percentile Sensitivity

We consider a class \mathcal{M} composed of two different configurations of a continuous gridworld domain with 2D states and 2D actions, which we call the *GridWorld with Slope*. In each configuration, the agent navigates through four rooms connected by narrow hallways, by choosing a (bounded) increment along the coordinate directions. A visual representation of the setting can be found in Figure 2a, where the shaded areas denote the initial state distribution and the arrows render a slope that favors or contrasts the agent’s movement. The configuration on the left has a south-facing slope, and thus it is called GridWorld with South slope (GWS). Instead, the one on the right is called GridWorld with North slope (GWN) as it has a north-facing slope. This class of environments is unbalanced (and thus interesting to our purpose) for two reasons: First, the GWN configuration is more challenging from a pure exploration standpoint, since the slope prevents the agent from easily reaching the two bottom rooms; secondly, the distribution over the class is also unbalanced, as it is $p_{\mathcal{M}} = [\text{Pr}(\text{GWS}), \text{Pr}(\text{GWN})] = [0.8, 0.2]$. In this setting, we compare α MEPOL against MEPOL (Mutti, Pratissoli, and Restelli 2021), which is akin to α MEPOL with $\alpha = 1$,¹ to highlight the importance of percentile sensitivity w.r.t. a naïve approach to the multiple-environments scenario. The methods are evaluated in terms of the state visitation entropy $\mathcal{E}_{\mathcal{M}}^1$ induced by the exploration strategies they learn.

In Figure 2, we compare the performance of the optimal exploration strategy obtained by running α MEPOL ($\alpha = 0.2$) and MEPOL for 150 epochs on the GridWorld with Slope class ($p_{\mathcal{M}} = [0.8, 0.2]$). We show that the two methods achieve a very similar expected performance over the class (Figure 2b). However, this expected performance is the result of a (weighted) average of very different contributions. As anticipated, MEPOL has a strong performance in GWS ($p_{\mathcal{M}} = [1, 0]$, Figure 2c), which is close to the configuration-specific optimum (dashed line), but it displays a bad showing in the adverse GWN ($p_{\mathcal{M}} = [0, 1]$, Figure 2d). Conversely,

¹The pseudocode is identical to Algorithm 1 except that all trajectories affect the gradient estimate in (5).

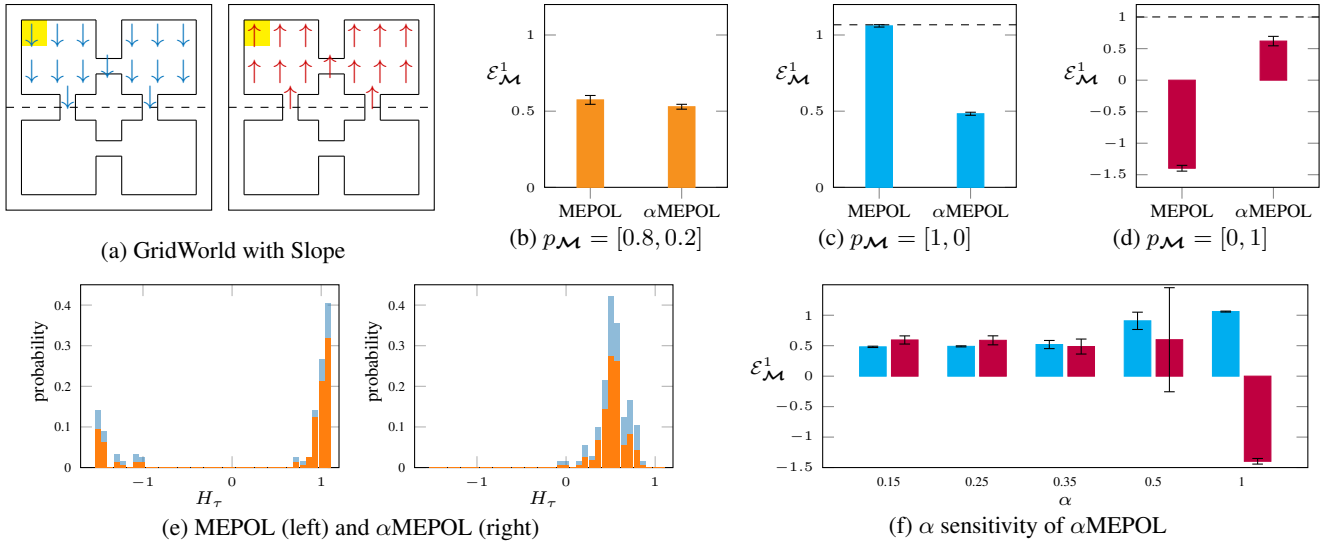


Figure 2: Pre-training performance $\varepsilon_{\mathcal{M}}^1$ obtained by α MEPOL ($\alpha = 0.2$) and MEPOL in the *GridWorld with Slope* domain (a). The policies are trained on (b) and tested on (b, c, d). The dashed lines in (c, d) represent the optimal performance. The empirical distribution having mean in (b) is reported in (e). The behaviour of α MEPOL with different α is reported in (f). For every plot, we provide 95% c.i. over 10 runs.

α MEPOL learns a strategy that is much more robust to the configuration, showing a similar performance in GWS and GWN, as the percentile sensitivity prioritizes the worst case during training. To confirm this conclusion, we look at the actual distribution that is generating the expected performance in Figure 2b. In Figure 2e, we provide the empirical distribution of the trajectory-wise performance (H_{τ}), considering a batch of 200 trajectories with $p_{\mathcal{M}} = [0.8, 0.2]$. It clearly shows that MEPOL is heavy-tailed towards lower outcomes, whereas α MEPOL concentrates around the mean. *This suggests that with a conservative choice of α we can induce a good exploration outcome for every trajectory (and any configuration), while without percentile sensitivity we cannot hedge against the risk of particularly bad outcomes.* However, let us point out that not all classes of environments would expose such an issue for a naïve, risk-neutral approach (see Appendix E.4 for a counterexample), but it is fair to assume that this would arguably generalize to any setting where there is an imbalance (either in the hardness of the configurations, or in their sampling probability) in the class. These are the settings we care about, as they require nuanced solutions (e.g., α MEPOL) for scenarios with multiple environments.

6.2 On the Value of the Percentile

In this section, we consider repeatedly training α MEPOL with different values of α in the GridWorld with Slope domain, and we compare the resulting exploration performance $\varepsilon_{\mathcal{M}}^1$ as before. In Figure 2f, we can see that the lower α we choose, the more we prioritize GWN (right bar for every α) at the expense of GWS (left bar). Note that this trend carries on with increasing α , ending in the values of Figures 2c, 2d. The reason for this behavior is quite straightforward, the smaller is α , the larger is the share of trajectories from the adverse configuration (GWN) ending up in the percentile at first, and

thus the more GWN affects the policy update (see the gradient in (5)). *Note that the value of the percentile α should not be intended as a hyper-parameter to tune via trial and error, but rather as a parameter to select the desired risk profile of the algorithm.* Indeed, there is not a way to say which of the outcomes in Figure 2f is preferable, as they are all reasonable trade-offs between the average and worst-case performance, which might be suited for specific applications. For the sake of consistency, in every experiment of our analysis we report results with a value of α that matches the sampling probability of the worst-case configuration, but similar arguments could be made for different choices of α .

6.3 Supervised Fine-Tuning

To assess the benefit of the pre-trained strategy, we design a family of MDPs \mathcal{M}^R , where $\mathcal{M} \in \{\text{GWS}, \text{GWN}\}$, and R is any sparse reward function that gives 1 when the agent reaches the area nearby a random goal location and 0 otherwise. On this family, we compare the performance achieved by TRPO (Schulman et al. 2015) with different initializations: The exploration strategies learned (as in Section 6.1) by α MEPOL ($\alpha = 0.2$) and MEPOL, or a randomly initialized policy (Random). These three variations are evaluated in terms of their average return $\mathcal{J}_{\mathcal{M}^R}$, which is defined in (1), over 50 randomly generated goal locations (Figure 3b). As expected, the performance of TRPO with MEPOL is competitive in the GWS configuration (Figure 3), but it falls sharply in the GWN configuration, where it is not significantly better than TRPO with Random. Instead, the performance of TRPO with α MEPOL is strong on both GWS and GWN. Despite the simplicity of the domain, solving an RL problem in GWN with an adverse goal location is far-fetched for both a random initialization and a naïve solution to the problem of unsupervised RL in multiple environments.

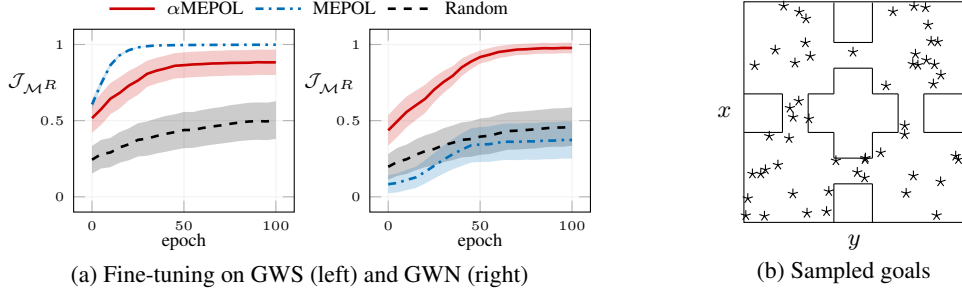


Figure 3: Fine-tuning performance $\mathcal{J}_{\mathcal{M}^R}$ as a function of learning epochs achieved by TRPO initialized with α MEPOL ($\alpha = 0.2$), MEPOL, and random exploration strategies, when dealing with a set of RL tasks specified on the *GridWorld with Slope* domain (a). We provide 95% c.i. over 50 randomly sampled goal locations (b).

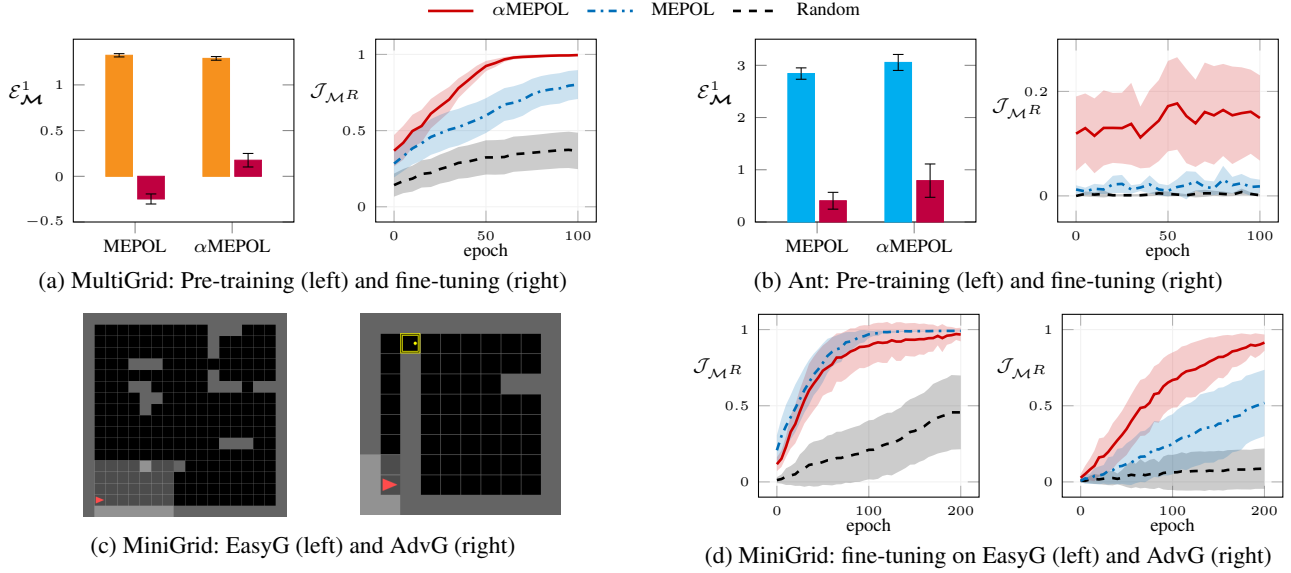


Figure 4: Pre-training performance $\mathcal{E}_{\mathcal{M}}^1$ (95% c.i. over 10 runs) achieved by α MEPOL ($\alpha = 0.1$ (a), $\alpha = 0.2$ (b)) and MEPOL in the *MultiGrid* (a) and *Ant* (b) domains. Fine-tuning performance $\mathcal{J}_{\mathcal{M}^R}$ (95% c.i. over 50 tasks (a), 8 tasks (b), 13 tasks (d)) obtained by TRPO with corresponding initialization (α MEPOL, MEPOL, Random), in the *MultiGrid* (a), *Ant* (b), and *MiniGrid* (d) domains. *MiniGrid* domains are illustrated in (c).

6.4 Scaling to Larger Classes of Environments

In this section, we consider a class \mathcal{M} composed of 10 different configurations of the continuous gridworlds presented in Section 6.1 (including the GWN as the worst-case configuration) which we call the *MultiGrid* domain. As before, we compare α MEPOL ($\alpha = 0.1$) and MEPOL on the exploration performance $\mathcal{E}_{\mathcal{M}}^1$ achieved by the optimal strategy, in this case considering a uniformly distributed $p_{\mathcal{M}}$. While the average performance of MEPOL is slightly higher across the class (Figure 4a left, left bar), α MEPOL still has a decisive advantage in the worst-case configuration (Figure 4a left, right bar). Just as in Section 6.3, this advantage transfer to the fine-tuning, where we compare the average return $\mathcal{J}_{\mathcal{M}^R}$ achieved by TRPO with α MEPOL, MEPOL, and Random initializations over 50 random goal locations in the GWN configuration (Figure 4a right). *Whereas in the following sections we will only consider classes of two environments, this*

experiment shows that the arguments made for small classes of environments can easily generalize to larger classes.

6.5 Scaling to Increasing Dimensions

In this section, we consider a class \mathcal{M} consisting of two Ant environments, with 29D states and 8D actions. In the first, sampled with probability $p_{\mathcal{M}_1} = 0.8$, the Ant faces a wide descending staircase (*Ant Stairs Down*). In the second, the Ant faces a narrow ascending staircase (*Ant Stairs Up*, sampled with probability $p_{\mathcal{M}_2} = 0.2$), which is significantly harder to explore than the former. In the mold of the gridworlds in Section 6.1, these two configurations are specifically designed to create an imbalance in the class. As in Section 6.1, we compare α MEPOL ($\alpha = 0.2$) against MEPOL on the exploration performance $\mathcal{E}_{\mathcal{M}}^1$ achieved after 500 epochs. α MEPOL fares slightly better than MEPOL both in the worst-case configuration (Figure 4b left, right bar) and,

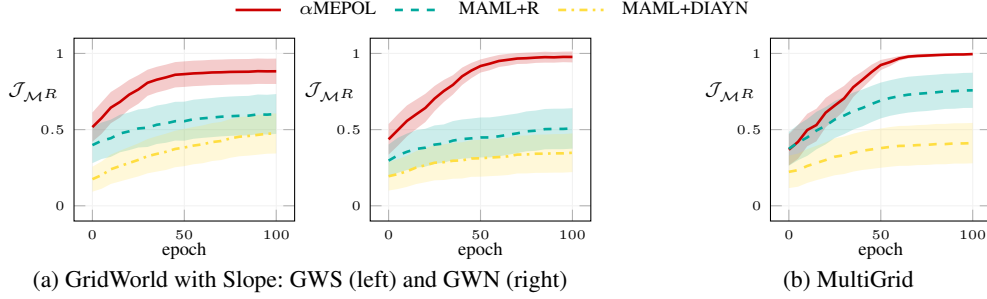


Figure 5: Fine-tuning performance $\mathcal{J}_{\mathcal{M}^R}$ achieved by TRPO initialized with α MEPOL ($\alpha = 0.2$ (a), $\alpha = 0.1$ (b)), a MAML+R meta-policy, and a MAML+DIAYN meta-policy, when dealing with a set of RL tasks in the *GridWorld with Slope* (a) and the *MultiGrid* (b) domains. We provide 95% c.i. over 50 tasks.

surprisingly, in the easier one (Figure 4b left, left bar).² Then, we design a set of incrementally challenging fine-tuning tasks in the *Ant Stairs Up*, which give reward 1 upon reaching a certain step of the staircase. Also in this setting, TRPO with α MEPOL initialization outperforms TRPO with MEPOL and Random in terms of the average return $\mathcal{J}_{\mathcal{M}^R}$ (Figure 4b right). Note that these sparse-reward continuous control tasks are particularly arduous: TRPO with MEPOL and Random barely learns anything, while even TRPO with α MEPOL does not handily reach the optimal average return (1).

6.6 Scaling to Visual Inputs

In this section, we consider a class \mathcal{M} of two partially-observable MiniGrid (Chevalier-Boisvert, Willems, and Pal 2018) environments, in which the observation is a 147D image of the agent’s field of view. In Figure 4c, we provide a visualization of the domain: The easier configuration (EasyG, left) is sampled with probability $p_{\mathcal{M}_1} = 0.8$, the adverse configuration (AdvG, right) is sampled with probability $p_{\mathcal{M}_2} = 0.2$. Two factors make the AdvG more challenging to explore, which are the presence of a door at the top-left of the grid, and reversing the effect of agent’s movements (e.g., the agent goes backward when it tries to go forward). Whereas in all the previous experiments we estimated the entropy on the raw input features, visual inputs require a wiser choice of a metric. As proposed in (Seo et al. 2021), we process the observations through a random encoder before computing the entropy estimate in (3), while keeping everything else as in Algorithm 1. We run this slightly modified version of α MEPOL ($\alpha = 0.2$) and MEPOL for 300 epochs. Then, we compare TRPO with the learned initializations (as well as Random) on sparse-reward fine-tuning tasks defined upon the class. As in previous settings, TRPO with α MEPOL results slightly worse than TRPO with MEPOL in the easier configuration (Figure 4d, left), but significantly better in the worst-case (Figure 4d, right). Notably, TRPO from scratch struggles to learn the tasks, especially in the AdvG (Figure 4d, right). *Although the MiniGrid domain is extremely simple*

²Note that this would not happen in general, as we expect α MEPOL to be better in the worst-case but worse on average. In this setting, the percentile sensitivity positively biases the average performance due to the peculiar structure of the environments.

from a vision standpoint, we note that the same architecture can be employed in more challenging scenarios (Seo et al. 2021), while the focus of this experiment is the combination between visual inputs and multiple environments.

6.7 Comparison with Meta-RL

In this section, we compare our approach against meta-training a policy with MAML (Finn, Abbeel, and Levine 2017) on the same *GridWorld with Slope* ($p_{\mathcal{M}} = [0.8, 0.2]$) and *MultiGrid* (uniformly distributed $p_{\mathcal{M}}$) domains that we have previously presented. Especially, we consider two relevant baselines. The first is MAML+R, to which we provide full access to the tasks (i.e., rewards) during meta-training. Note that this gives MAML+R an edge over α MEPOL, which operates reward-free training. The second is MAML+DIAYN (Gupta et al. 2018a), which operates unsupervised meta-training through an intrinsic reward function learned with DIAYN (Eysenbach et al. 2018). As in previous sections, we consider the average return $\mathcal{J}_{\mathcal{M}^R}$ achieved by TRPO initialized with the exploration strategy learned by α MEPOL or the meta-policy learned by MAML+R and MAML+DIAYN. TRPO with α MEPOL fares clearly better than TRPO with the meta-policies in all the configurations (Figures 5a, 5b). Even if it works fine in fast adaptation (see Appendix E.5), *MAML struggles to encode the diversity of task distribution into a single meta-policy and to deal with the most adverse tasks in the long run*. Moreover, DIAYN does not specifically handle multiple environments, and it fails to cope with the larger *MultiGrid* class.

7 Conclusions

In this paper, we addressed the problem of unsupervised RL in a class of multiple environments. First, we formulated the problem within a tractable objective, which is inspired by MSVE but includes an additional percentile sensitivity. Then, we presented a policy gradient algorithm, α MEPOL, to optimize this objective. Finally, we provided an extensive experimental analysis to show its ability in the unsupervised pre-training and the benefits it brings to the subsequent supervised fine-tuning. We believe that this paper motivates the importance of designing specific solutions to the relevant problem of unsupervised RL in multiple environments.

References

- Achiam, J.; Edwards, H.; Amodei, D.; and Abbeel, P. 2018. Variational option discovery algorithms. *arXiv preprint arXiv:1807.10299*.
- Ajgl, J.; and Šimandl, M. 2011. Differential entropy estimation by particles. *IFAC Proceedings Volumes*.
- Bellemare, M.; Srinivasan, S.; Ostrovski, G.; Schaul, T.; Sutton, D.; and Munos, R. 2016. Unifying count-based exploration and intrinsic motivation. *Advances in Neural Information Processing Systems*.
- Burda, Y.; Edwards, H.; Storkey, A.; and Klimov, O. 2019. Exploration by random network distillation. In *International Conference on Learning Representations*.
- Campos, V.; Sprechmann, P.; Hansen, S.; Barreto, A.; Kapturowski, S.; Vitvitskyi, A.; Badia, A. P.; and Blundell, C. 2021. Beyond fine-tuning: Transferring behavior in reinforcement learning. *arXiv preprint arXiv:2102.13515*.
- Chevalier-Boisvert, M.; Willems, L.; and Pal, S. 2018. Minimalistic gridworld environment for openai gym. *GitHub repository*.
- Chow, Y.; and Ghavamzadeh, M. 2014. Algorithms for CVaR optimization in MDPs. In *Advances in neural information processing systems*.
- Csiszár, I.; and Talata, Z. 2006. Context tree estimation for not necessarily finite memory processes, via BIC and MDL. *IEEE Transactions on Information theory*.
- Deisenroth, M.; Neumann, G.; and Peters, J. 2013. A survey on policy search for robotics. *Foundations and Trends in Robotics*.
- Duan, Y.; Chen, X.; Houthoofd, R.; Schulman, J.; and Abbeel, P. 2016. Benchmarking deep reinforcement learning for continuous control. In *Proceedings of the International Conference on Machine Learning*.
- Eysenbach, B.; Gupta, A.; Ibarz, J.; and Levine, S. 2018. Diversity is all you need: Learning skills without a reward function. In *International Conference on Learning Representations*.
- Finn, C.; Abbeel, P.; and Levine, S. 2017. Model-agnostic meta-learning for fast adaptation of deep networks. In *Proceedings of the International Conference on Machine Learning*.
- Gregor, K.; Rezende, D. J.; and Wierstra, D. 2016. Variational intrinsic control. *arXiv preprint arXiv:1611.07507*.
- Guo, Z. D.; Azar, M. G.; Saade, A.; Thakoor, S.; Piot, B.; Pires, B. A.; Valko, M.; Mesnard, T.; Lattimore, T.; and Munos, R. 2021. Geometric entropic exploration. *arXiv preprint arXiv:2101.02055*.
- Gupta, A.; Eysenbach, B.; Finn, C.; and Levine, S. 2018a. Unsupervised meta-learning for reinforcement learning. *arXiv preprint arXiv:1806.04640*.
- Gupta, A.; Mendonca, R.; Liu, Y.; Abbeel, P.; and Levine, S. 2018b. Meta-reinforcement learning of structured exploration strategies. In *Advances in Neural Information Processing Systems*.
- Hallak, A.; Di Castro, D.; and Mannor, S. 2015. Contextual Markov decision processes. *arXiv preprint arXiv:1502.02259*.
- Hazan, E.; Kakade, S.; Singh, K.; and Van Soest, A. 2019. Provably efficient maximum entropy exploration. In *Proceedings of the International Conference on Machine Learning*.
- Jin, C.; Krishnamurthy, A.; Simchowitz, M.; and Yu, T. 2020. Reward-free exploration for reinforcement learning. In *Proceedings of the International Conference on Machine Learning*.
- Kolla, R. K.; Prashanth, L.; Bhat, S. P.; and Jagannathan, K. 2019. Concentration bounds for empirical conditional value-at-risk: The unbounded case. *Operations research letters*.
- Kwon, J.; Efroni, Y.; Caramanis, C.; and Mannor, S. 2021. RL for latent MDPs: Regret guarantees and a lower bound. In *Advances in Neural Information Processing Systems*.
- L.A., P.; Jagannathan, K.; and Kolla, R. 2020. Concentration bounds for CVaR estimation: The cases of light-tailed and heavy-tailed distributions. In *Proceedings of the International Conference on Machine Learning*.
- Laskin, M.; Yarats, D.; Liu, H.; Lee, K.; Zhan, A.; Lu, K.; Cang, C.; Pinto, L.; and Abbeel, P. 2021. URLB: Unsupervised reinforcement learning benchmark. In *Conference on Neural Information Processing Systems Datasets and Benchmarks Track (Round 2)*.
- Lee, L.; Eysenbach, B.; Parisotto, E.; Xing, E.; Levine, S.; and Salakhutdinov, R. 2019. Efficient exploration via state marginal matching. *arXiv preprint arXiv:1906.05274*.
- Liu, H.; and Abbeel, P. 2021a. Aps: Active pretraining with successor features. In *Proceedings of the International Conference on Machine Learning*.
- Liu, H.; and Abbeel, P. 2021b. Behavior from the void: Unsupervised active pre-training. In *Advances in Neural Information Processing Systems*.
- Metelli, A. M.; Mutti, M.; and Restelli, M. 2018. Configurable Markov decision processes. In *Proceedings of the International Conference on Machine Learning*.
- Metelli, A. M.; Papini, M.; Faccio, F.; and Restelli, M. 2018. Policy optimization via importance sampling. In *Advances in Neural Information Processing Systems*.
- Mutti, M.; Pratissoli, L.; and Restelli, M. 2021. Task-agnostic exploration via policy gradient of a non-parametric state entropy estimate. In *Proceedings of the AAAI Conference on Artificial Intelligence*.
- Mutti, M.; and Restelli, M. 2020. An intrinsically-motivated approach for learning highly exploring and fast mixing policies. In *Proceedings of the AAAI Conference on Artificial Intelligence*.
- Ostrovski, G.; Bellemare, M. G.; Oord, A.; and Munos, R. 2017. Count-based exploration with neural density models. In *International Conference on Machine Learning*.
- Parisi, S.; Dean, V.; Pathak, D.; and Gupta, A. 2021. Interesting object, curious agent: Learning task-agnostic exploration. In *Advances in Neural Information Processing Systems*.

- Parisi, S.; Pirotta, M.; and Restelli, M. 2016. Multi-objective reinforcement learning through continuous pareto manifold approximation. *Journal of Artificial Intelligence Research*.
- Pathak, D.; Agrawal, P.; Efros, A. A.; and Darrell, T. 2017. Curiosity-driven exploration by self-supervised prediction. In *Proceedings of the International Conference on Machine Learning*.
- Pathak, D.; Gandhi, D.; and Gupta, A. 2019. Self-supervised exploration via disagreement. In *Proceedings of the International Conference on Machine Learning*.
- Pirotta, M.; Restelli, M.; and Bascetta, L. 2015. Policy gradient in Lipschitz Markov decision processes. *Machine Learning*.
- Puterman, M. L. 2014. *Markov decision processes: Discrete stochastic dynamic programming*. John Wiley & Sons.
- Rajendran, J.; Lewis, R.; Veeriah, V.; Lee, H.; and Singh, S. 2020. How should an agent practice? In *Proceedings of the AAAI Conference on Artificial Intelligence*.
- Rajeswaran, A.; Ghotra, S.; Ravindran, B.; and Levine, S. 2016. EPOpt: Learning robust neural network policies using model ensembles. In *Proceedings of the International Conference on Learning Representations*.
- Rockafellar, R. T.; Uryasev, S.; et al. 2000. Optimization of conditional value-at-risk. *Journal of risk*.
- Satia, J. K.; and Lave Jr, R. E. 1973. Markovian decision processes with uncertain transition probabilities. *Operations Research*.
- Schmidhuber, J. 1991. A possibility for implementing curiosity and boredom in model-building neural controllers. In *Proceedings of the International Conference on Simulation of Adaptive Behavior: From Animals to Animats*.
- Schulman, J.; Levine, S.; Abbeel, P.; Jordan, M.; and Moritz, P. 2015. Trust region policy optimization. In *Proceedings of the International Conference on Machine Learning*.
- Seo, Y.; Chen, L.; Shin, J.; Lee, H.; Abbeel, P.; and Lee, K. 2021. State entropy maximization with random encoders for efficient exploration. In *Proceedings of the International Conference on Machine Learning*.
- Shannon, C. E. 1948. A mathematical theory of communication. *The Bell system technical journal*.
- Singh, H.; Misra, N.; Hnizdo, V.; Fedorowicz, A.; and Demchuk, E. 2003. Nearest neighbor estimates of entropy. *American journal of mathematical and management sciences*.
- Sutton, R. S.; and Barto, A. G. 2018. *Reinforcement learning: An introduction*. MIT press.
- Tamar, A.; Glassner, Y.; and Mannor, S. 2015. Optimizing the CVaR via sampling. In *Proceedings of the AAAI Conference on Artificial Intelligence*.
- Tang, H.; Houthoofd, R.; Foote, D.; Stooke, A.; Chen, X.; Duan, Y.; Schulman, J.; De Turck, F.; and Abbeel, P. 2017. # exploration: A study of count-based exploration for deep reinforcement learning. In *Advances in Neural Information Processing Systems*.
- Tarbouriech, J.; and Lazaric, A. 2019. Active exploration in Markov decision processes. In *Proceedings of the International Conference on Artificial Intelligence and Statistics*.
- Villani, C. 2008. *Optimal transport: old and new*. Springer Science & Business Media.
- Xu, T.; Liu, Q.; Zhao, L.; and Peng, J. 2018. Learning to explore via meta-policy gradient. In *Proceedings of the International Conference on Machine Learning*.
- Yarats, D.; Fergus, R.; Lazaric, A.; and Pinto, L. 2021. Reinforcement learning with prototypical representations. In *Proceedings of the International Conference on Machine Learning*.
- Zhang, C.; Cai, Y.; and Li, L. H. J. 2021. Exploration by maximizing Rényi entropy for reward-free RL framework. In *Proceedings of the AAAI Conference on Artificial Intelligence*.
- Zhang, X.; Ma, Y.; and Singla, A. 2020. Task-agnostic exploration in reinforcement learning. In *Advances in Neural Information Processing Systems*.
- Zintgraf, L.; Shiarlis, K.; Igl, M.; Schulze, S.; Gal, Y.; Hofmann, K.; and Whiteson, S. 2019. VariBAD: A very good method for bayes-adaptive deep RL via meta-learning. In *Proceedings of the International Conference on Learning Representations*.

A Relevant Literature

Our work lies at the intersection of unsupervised RL, robust and risk-averse in RL, and meta-RL. We revise below the relevant literature in these three fields. Other problem formulations that have similarities with ours are the *reward-free RL* (Jin et al. 2020) and *task-agnostic RL* (Zhang, Ma, and Singla 2020). These frameworks also consider an unsupervised exploration phase (i.e., without rewards). Differently from unsupervised RL, the objective of the exploration is to allow the agent to plan for an ϵ -optimal policy for the worst-case reward (reward-free RL) or an oblivious reward (task-agnostic RL), i.e., they do not consider a fine-tuning phase. Hence, the unsupervised exploration focuses on the coverage of the collected data rather than the performance of the pre-trained policy. Moreover, the existing works only consider single-environment settings. Another formulation that relates to ours is the *latent MDP* setting (Hallak, Di Castro, and Mannor 2015; Kwon et al. 2021), in which the agent sequentially interact with an MDP drawn from a fixed distribution, similarly to our unsupervised pre-training phase. However, they assume supervised interactions with the class of environments, and they pursue regret minimization rather than policy pre-training.

Unsupervised RL The literature that relates the most with our work is the one pursuing unsupervised RL in a single environment. A complete survey of the existing works along with an empirical comparison of the main methods can be found in (Laskin et al. 2021). Here, we report a brief summary. Laskin et al. (2021) group the existing methods in three categories: Knowledge-based, data-based, and competence-based. The knowledge-based methods (Schmidhuber 1991; Pathak et al. 2017; Burda et al. 2019; Pathak, Gandhi, and Gupta 2019) are those that exploit the unsupervised pre-training to acquire useful knowledge about the environment. The pre-training objective is usually proportional to the prediction error of a learned model. Instead, the data-based methods try to maximize the diversity of the collected samples, for which count-based bonuses (Bellemare et al. 2016; Ostrovski et al. 2017; Tang et al. 2017) and MSVE are typical pre-training objectives. Some of the MSVE methods (Hazan et al. 2019; Lee et al. 2019) focus on learning a mixture of policies that is collectively MSVE optimal, while other (Tarbouriech and Lazaric 2019; Mutti and Restelli 2020) casts the MSVE as a dual (or surrogate) linear program in tabular settings. Successive works tackle MSVE at scale with non-parametric entropy estimation (Mutti, Pratissoli, and Restelli 2021; Liu and Abbeel 2021b,a; Yarats et al. 2021; Seo et al. 2021), or introduce variations to the entropy objective, such as geometry-awareness (Guo et al. 2021) and Rényi generalization (Zhang, Cai, and Li 2021). Finally, competence-based methods, which include (Gregor, Rezende, and Wierstra 2016; Eysenbach et al. 2018; Achiam et al. 2018) and to some extent (Lee et al. 2019; Liu and Abbeel 2021a), make use of the unsupervised pre-training to acquire a set of useful skills. Their pre-training objective is usually related to the mutual information between a latent skill vector and the state visitation induced by the skill. To the best of our knowledge, all the existing solutions to the unsupervised RL problem are environment-specific (with the exception of (Parisi et al. 2021) commented in Section 2) and do not directly address the multiple-environments setting.

Robust RL and Risk-Aversion Previous work considered *CVaR optimization* in RL as we do, either to learn a policy that is averse to the risk induced by the volatility of the returns (Tamar, Glassner, and Mannor 2015; Chow and Ghavamzadeh 2014) or by changes in the environment dynamics (e.g., Rajeswaran et al. 2016). Here we account for a different source of risk, which is the one of running into a particularly unfavorable environment for the pre-trained exploration strategy.

Meta-RL As we mentioned in Section 2, our framework resembles the *meta-RL* setting (Finn, Abbeel, and Levine 2017), in which we would call *meta-training* the unsupervised pre-training, and *meta-testing* the supervised fine-tuning. While some methods target exploration in meta-RL (e.g., Xu et al. 2018; Gupta et al. 2018b; Zintgraf et al. 2019), they usually assume access to rewards during meta-training, with the notable exception of (Gupta et al. 2018a). To the best of our knowledge, none of the existing works combine reward-free meta-training with a multiple-environments setting.

B Preliminary Theoretical Analysis of the Problem

We aim to theoretically analyze the problem in (2), and especially, what makes a class of multiple CMPs hard to explore with a unique strategy. This has to be intended as a preliminary discussion on the problem, which could serve as a starting point for future works, rather than a thorough theoretical characterization. First, it is worth introducing some additional notation.

Lipschitz Continuity Let X, Y be two metric sets with metric functions d_X, d_Y . We say a function $f : X \rightarrow Y$ is L_f -Lipschitz continuous if it holds for some constant L_f

$$d_Y(f(x'), f(x)) \leq L_f d_X(x', x), \forall (x', x) \in X^2,$$

where the smallest L_f is the Lipschitz constant and the Lipschitz semi-norm is $\|f\|_L = \sup_{x', x \in X} \left\{ \frac{d_Y(f(x'), f(x))}{d_X(x', x)} : x' \neq x \right\}$. When dealing with probability distributions we need to introduce a proper metric. Let p, q be two probability measures, we will either consider the Wasserstein metric (Villani 2008), defined as

$$d_{W_1}(p, q) = \sup_f \left\{ \left| \int_X f(x)(p(x) - q(x)) dx \right| : \|f\|_L \leq 1 \right\},$$

or the Total Variation (TV) metric, defined as

$$d_{TV}(p, q) = \frac{1}{2} \int_X |p(x) - q(x)| dx.$$

Intuitively, learning to explore a class \mathcal{M} with a policy π is challenging when the state distributions induced by π in different $\mathcal{M} \in \mathcal{M}$ are diverse. The more diverse they are, the more their entropy can vary, and the harder is to get a π with a large entropy across the class. To measure this diversity, we are interested in the supremum over the distances between the state distributions $(d_\pi^{\mathcal{M}_1}, \dots, d_\pi^{\mathcal{M}_I})$ that a single policy $\pi \in \Pi$ realizes over the class \mathcal{M} . We call this measure the *diameter* $\mathcal{D}_{\mathcal{M}}$ of the class \mathcal{M} . Since we have infinitely many policies in Π , computing $\mathcal{D}_{\mathcal{M}}$ is particularly arduous. However, we are able to provide an upper bound to $\mathcal{D}_{\mathcal{M}}$ defined through a Wasserstein metric.

Assumption 1. Let $d_{\mathcal{S}}$ be a metric on \mathcal{S} . The class \mathcal{M} is L_{P^π} -Lipschitz continuous,

$$d_{W_1}(P^\pi(\cdot|s'), P^\pi(\cdot|s)) \leq L_{P^\pi} d_{\mathcal{S}}(s', s), \quad \forall (s', s) \in \mathcal{S}^2,$$

where $P^\pi(s|\bar{s}) = \int_{\mathcal{A}} \pi(\bar{a}|\bar{s}) P(s|\bar{s}, \bar{a}) d\bar{a}$ for $P \in \mathcal{M}$, $\pi \in \Pi$, L_{P^π} is a constant $L_{P^\pi} < 1$.

Theorem B.1. Let \mathcal{M} be a class of CMPs satisfying Ass. 1. Let $d_\pi^{\mathcal{M}}$ be the marginal state distribution over T steps induced by the policy π in $\mathcal{M} \in \mathcal{M}$. We can upper bound the diameter $\mathcal{D}_{\mathcal{M}}$ as

$$\mathcal{D}_{\mathcal{M}} := \sup_{\pi \in \Pi, \mathcal{M}', \mathcal{M} \in \mathcal{M}} d_{W_1}(d_\pi^{\mathcal{M}'}, d_\pi^{\mathcal{M}}) \leq \sup_{P', P \in \mathcal{M}} \frac{1 - L_{P^\pi}^T}{1 - L_{P^\pi}} \sup_{s \in \mathcal{S}, a \in \mathcal{A}} d_{W_1}(P'(\cdot|s, a), P(\cdot|s, a)).$$

Theorem B.1 provides a measure to quantify the hardness of the exploration problem in a specific class of CMPs, and to possibly compare one class with another. However, the value of $\mathcal{D}_{\mathcal{M}}$ might result, due to the supremum over Π , from a policy that is far away from the policies we actually deploy while learning, say $(\pi_0, \dots, \pi_{\mathcal{E}}^*)$. To get a finer assessment of the hardness of \mathcal{M} we face in practice, it is worth considering a policy-specific measure to track during the optimization. We call this measure the π -diameter $\mathcal{D}_{\mathcal{M}}(\pi)$ of the class \mathcal{M} . Theorem B.2 provides an upper bound to $\mathcal{D}_{\mathcal{M}}(\pi)$ defined through a convenient TV metric.

Theorem B.2. Let \mathcal{M} be a class of CMPs, let $\pi \in \Pi$ be a policy, and let $d_\pi^{\mathcal{M}}$ be the marginal state distribution over T steps induced by π in $\mathcal{M} \in \mathcal{M}$. We can upper bound the π -diameter $\mathcal{D}_{\mathcal{M}}(\pi)$ as

$$\mathcal{D}_{\mathcal{M}}(\pi) := \sup_{\mathcal{M}', \mathcal{M} \in \mathcal{M}} d_{TV}(d_\pi^{\mathcal{M}'}, d_\pi^{\mathcal{M}}) \leq \sup_{P', P \in \mathcal{M}} T \mathbb{E}_{\substack{s \sim d_\pi^{\mathcal{M}} \\ a \sim \pi(\cdot|s)}} d_{TV}(P'(\cdot|s, a), P(\cdot|s, a)).$$

The last missing piece we aim to derive is a result to relate the π -diameter $\mathcal{D}_{\mathcal{M}}(\pi)$ of the class \mathcal{M} (Theorem B.2) with the actual exploration objective, i.e., the entropy of the state visitations induced by the policy π over the environments in the class. In the following theorem, we provide an upper bound to the *entropy gap* induced by the policy π within the class \mathcal{M} .

Theorem B.3. Let \mathcal{M} be a class of CMPs, let $\pi \in \Pi$ be a policy and $\mathcal{D}_{\mathcal{M}}(\pi)$ the corresponding π -diameter of \mathcal{M} . Let $d_\pi^{\mathcal{M}}$ be the marginal state distribution over T steps induced by π in $\mathcal{M} \in \mathcal{M}$, and let $\sigma_{\mathcal{M}} \leq \sigma_{\mathcal{M}} := \inf_{s \in \mathcal{S}} d_\pi^{\mathcal{M}}(s), \forall \mathcal{M} \in \mathcal{M}$. We can upper bound the entropy gap of the policy π within the model class \mathcal{M} as

$$\sup_{\mathcal{M}', \mathcal{M} \in \mathcal{M}} |H(d_\pi^{\mathcal{M}'}) - H(d_\pi^{\mathcal{M}})| \leq (\mathcal{D}_{\mathcal{M}}(\pi))^2 / \sigma_{\mathcal{M}} + \mathcal{D}_{\mathcal{M}}(\pi) \log(1/\sigma_{\mathcal{M}})$$

C Proofs

Proposition 5.1. The policy gradient of the exploration objective $\mathcal{E}_{\mathcal{M}}^\alpha(\pi_\theta)$ w.r.t. θ is given by

$$\begin{aligned} \nabla_\theta \mathcal{E}_{\mathcal{M}}^\alpha(\pi_\theta) &= \mathbb{E}_{\substack{\mathcal{M} \sim p_{\mathcal{M}} \\ \tau \sim p_{\pi_\theta, \mathcal{M}}}} \left[\left(\sum_{t=0}^{T-1} \nabla_\theta \log \pi_\theta(a_{t,\tau} | s_{t,\tau}) \right) \right. \\ &\quad \left. \times \left(H_\tau - \text{VaR}_\alpha(H_\tau) \right) \middle| H_\tau \leq \text{VaR}_\alpha(H_\tau) \right]. \end{aligned}$$

Proof. Let us start from expanding the exploration objective (2) to write

$$\begin{aligned} \mathcal{E}_{\mathcal{M}}^\alpha(\pi) &= \text{CVaR}_\alpha(H_\tau) \\ &= \mathbb{E}_{\substack{\mathcal{M} \sim p_{\mathcal{M}} \\ \tau \sim p_{\pi, \mathcal{M}}}} [H_\tau \mid H_\tau \leq \text{VaR}_\alpha(H_\tau)] = \frac{1}{\alpha} \int_{-\infty}^{\text{VaR}_\alpha(H_\tau)} p_{\pi_\theta, \mathcal{M}}(h) h \, dh, \end{aligned} \tag{6}$$

where $p_{\pi_\theta, \mathcal{M}}$ is the probability density function (pdf) of the random variable H_τ when the policy π_θ is deployed on the class of environments \mathcal{M} , and the last equality comes from the definition of CVaR (Rockafellar, Uryasev et al. 2000). Before computing the gradient of (6), we derive a preliminary result for later use, i.e.,

$$\begin{aligned} \nabla_\theta \int_{-\infty}^{\text{VaR}_\alpha(H_\tau)} p_{\pi_\theta, \mathcal{M}}(h) dh \\ = \int_{-\infty}^{\text{VaR}_\alpha(H_\tau)} \nabla_\theta p_{\pi_\theta, \mathcal{M}}(h) dh + \nabla_\theta \text{VaR}_\alpha(H_\tau) p_{\pi_\theta, \mathcal{M}}(\text{VaR}_\alpha(H_\tau)) = 0, \end{aligned} \quad (7)$$

which follows directly from the Leibniz integral rule, noting that $\text{VaR}_\alpha(H_\tau)$ depends on θ through the pdf of H_τ . We now take the gradient of (6) to get

$$\begin{aligned} \nabla_\theta \mathcal{E}_\mathcal{M}^\alpha(\pi) \\ = \nabla_\theta \frac{1}{\alpha} \int_{-\infty}^{\text{VaR}_\alpha(H_\tau)} p_{\pi_\theta, \mathcal{M}}(h) h dh \\ = \frac{1}{\alpha} \int_{-\infty}^{\text{VaR}_\alpha(H_\tau)} \nabla_\theta p_{\pi_\theta, \mathcal{M}}(h) h dh + \frac{1}{\alpha} \nabla_\theta \text{VaR}_\alpha(H_\tau) \text{VaR}_\alpha(H_\tau) p_{\pi_\theta, \mathcal{M}}(\text{VaR}_\alpha(H_\tau)) \end{aligned} \quad (8)$$

$$= \frac{1}{\alpha} \int_{-\infty}^{\text{VaR}_\alpha(H_\tau)} \nabla_\theta p_{\pi_\theta, \mathcal{M}}(h) \left(h - \text{VaR}_\alpha(H_\tau) \right) dh, \quad (9)$$

where (8) follows from the Leibniz integral rule, and (9) is obtained from (8) through (7), which we can rearrange to write $p_{\pi_\theta, \mathcal{M}}(\text{VaR}_\alpha(H_\tau)) = \frac{1}{\nabla_\theta \text{VaR}_\alpha(H_\tau)} \int_{-\infty}^{\text{VaR}_\alpha(H_\tau)} \nabla_\theta p_{\pi_\theta, \mathcal{M}}(h) dh$. All of the steps above are straightforward replications of the derivations by Tamar et al. (Tamar, Glassner, and Mannor 2015), Proposition 1. To conclude the proof we just have to compute the term $\nabla_\theta p_{\pi_\theta, \mathcal{M}}(h)$, which is specific to our setting. Especially, we note that

$$\begin{aligned} \nabla_\theta p_{\pi_\theta, \mathcal{M}}(h) \\ = \int_{\mathcal{M}} p_{\mathcal{M}}(\mathcal{M}) \int_{\mathcal{T}} \nabla_\theta p_{\pi_\theta, \mathcal{M}}(\tau) \delta(h - H_\tau) d\tau d\mathcal{M} \end{aligned} \quad (10)$$

$$\begin{aligned} = \int_{\mathcal{M}} p_{\mathcal{M}}(\mathcal{M}) \int_{\mathcal{T}} p_{\pi_\theta, \mathcal{M}}(\tau) \nabla_\theta \log p_{\pi_\theta, \mathcal{M}}(\tau) \delta(h - H_\tau) d\tau d\mathcal{M} \\ = \int_{\mathcal{M}} p_{\mathcal{M}}(\mathcal{M}) \int_{\mathcal{T}} p_{\pi_\theta, \mathcal{M}}(\tau) \left(\sum_{t=0}^{T-1} \nabla_\theta \log \pi_\theta(a_{t,\tau} | s_{t,\tau}) \right) \delta(h - H_\tau) d\tau d\mathcal{M}, \end{aligned} \quad (11)$$

where (10) and (11) are straightforward from the definitions in Section 3, and \mathcal{T} is the set of feasible trajectories of length T . Finally, the result follows by plugging (11) into (9), which gives

$$\begin{aligned} \nabla_\theta \mathcal{E}_\mathcal{M}^\alpha(\pi) &= \frac{1}{\alpha} \int_{\mathcal{M}} p_{\mathcal{M}}(\mathcal{M}) \int_{\mathcal{T}} p_{\pi_\theta, \mathcal{M}}(\tau) \\ &\quad \times \int_{-\infty}^{\text{VaR}_\alpha(H_\tau)} \delta(h - H_\tau) \left(\sum_{t=0}^{T-1} \nabla_\theta \log \pi_\theta(a_{t,\tau} | s_{t,\tau}) \right) \left(h - \text{VaR}_\alpha(H_\tau) \right) dh d\tau d\mathcal{M}. \end{aligned}$$

□

Theorem B.1. Let \mathcal{M} be a class of CMPs satisfying Ass. 1. Let $d_\pi^\mathcal{M}$ be the marginal state distribution over T steps induced by the policy π in $\mathcal{M} \in \mathcal{M}$. We can upper bound the diameter $\mathcal{D}_\mathcal{M}$ as

$$\mathcal{D}_\mathcal{M} := \sup_{\pi \in \Pi, \mathcal{M}', \mathcal{M} \in \mathcal{M}} d_{W_1}(d_\pi^{\mathcal{M}'}, d_\pi^\mathcal{M}) \leq \sup_{P', P \in \mathcal{P}} \frac{1 - L_{P^\pi}^T}{1 - L_{P^\pi}} \sup_{s \in \mathcal{S}, a \in \mathcal{A}} d_{W_1}(P'(\cdot | s, a), P(\cdot | s, a)).$$

Proof. The proof follows techniques from (Pirodda, Restelli, and Bascetta 2015). Let us report a preliminary result which states that the function $h_f(\bar{s}) = \int_{\mathcal{A}} \pi(\bar{a} | \bar{s}) \int_{\mathcal{S}} P(s | \bar{s}, \bar{a}) ds d\bar{a}$ has a Lipschitz constant equal to L_{P^π} (Pirodda, Restelli, and Bascetta 2015, Lemma 3):

$$\begin{aligned} |h_f(\bar{s}') - h_f(\bar{s})| &= \left| \int_{\mathcal{S}} f(s) \int_{\mathcal{A}} \pi(a | \bar{s}') P(s | \bar{s}', a) da ds - \int_{\mathcal{S}} f(s) \int_{\mathcal{A}} \pi(a | \bar{s}) P(s | \bar{s}, a) da ds \right| \\ &= \left| \int_{\mathcal{S}} f(s) \left(P^\pi(s | \bar{s}') - P^\pi(s | \bar{s}) \right) ds \right| \leq L_{P^\pi} d_{\mathcal{S}}(\bar{s}', \bar{s}), \end{aligned} \quad (12)$$

where d_S is a metric over \mathcal{S} and $P^\pi(s|\bar{s}) = \int_{\mathcal{A}} \pi(\bar{a}|\bar{s})P(s|\bar{s}, \bar{a}) d\bar{a}$. Then, we note that the marginal state distribution over T steps $d_\pi^\mathcal{M}$ can be written as a sum of the contributions $d_{\pi,t}^\mathcal{M}$ related to any time step $t \in [T]$, which is

$$d_\pi^\mathcal{M}(s) = \frac{1}{T} \sum_{t=0}^{T-1} d_{\pi,t}^\mathcal{M}(s). \quad (13)$$

Hence, we can look at the Wasserstein distance of the state distributions for some $t \in [T]$ and $\mathcal{M}', \mathcal{M} \in \mathcal{M}$. We obtain

$$d_{W_1}(d_{\pi,t}^{\mathcal{M}'}, d_{\pi,t}^{\mathcal{M}}) = \sup_f \left\{ \left| \int_{\mathcal{S}} \left(d_{\pi,t}^{\mathcal{M}'}(s) - d_{\pi,t}^{\mathcal{M}}(s) \right) f(s) ds \right| : \|f\|_L \leq 1 \right\} \quad (14)$$

$$= \sup_f \left\{ \left| \int_{\mathcal{S}} \int_{\mathcal{A}} \int_{\mathcal{S}} \left(d_{\pi,t-1}^{\mathcal{M}'}(\bar{s}) \pi(\bar{a}|\bar{s}) P'(s|\bar{s}, \bar{a}) - d_{\pi,t-1}^{\mathcal{M}}(\bar{s}) \pi(\bar{a}|\bar{s}) P(s|\bar{s}, \bar{a}) \right) f(s) ds d\bar{a} d\bar{s} \right| : \|f\|_L \leq 1 \right\} \quad (15)$$

$$= \sup_f \left\{ \left| \int_{\mathcal{S}} d_{\pi,t-1}^{\mathcal{M}'}(\bar{s}) \int_{\mathcal{A}} \int_{\mathcal{S}} \pi(\bar{a}|\bar{s}) \left(P'(s|\bar{s}, \bar{a}) - P(s|\bar{s}, \bar{a}) \right) f(s) ds d\bar{a} d\bar{s} \right. \right. \\ \left. \left. + \int_{\mathcal{S}} \left(d_{\pi,t-1}^{\mathcal{M}'}(\bar{s}) - d_{\pi,t-1}^{\mathcal{M}}(\bar{s}) \right) \int_{\mathcal{A}} \int_{\mathcal{S}} \pi(\bar{a}|\bar{s}) P(s|\bar{s}, \bar{a}) f(s) ds d\bar{a} d\bar{s} \right| : \|f\|_L \leq 1 \right\} \quad (16)$$

$$\leq \sup_f \left\{ \left| \int_{\mathcal{S}} d_{\pi,t-1}^{\mathcal{M}'}(\bar{s}) \int_{\mathcal{A}} \int_{\mathcal{S}} \pi(\bar{a}|\bar{s}) \left(P'(s|\bar{s}, \bar{a}) - P(s|\bar{s}, \bar{a}) \right) f(s) ds d\bar{a} d\bar{s} \right| : \|f\|_L \leq 1 \right\} \\ + \sup_f \left\{ \left| \int_{\mathcal{S}} \left(d_{\pi,t-1}^{\mathcal{M}'}(\bar{s}) - d_{\pi,t-1}^{\mathcal{M}}(\bar{s}) \right) \int_{\mathcal{A}} \int_{\mathcal{S}} \pi(\bar{a}|\bar{s}) P(s|\bar{s}, \bar{a}) f(s) ds d\bar{a} d\bar{s} \right| : \|f\|_L \leq 1 \right\} \\ \leq \sup_f \left\{ \left| \int_{\mathcal{S}} d_{\pi,t-1}^{\mathcal{M}'}(\bar{s}) \int_{\mathcal{A}} \pi(\bar{a}|\bar{s}) d\bar{a} d\bar{s} \sup_{\bar{s} \in \mathcal{S}, \bar{a} \in \mathcal{A}} \left\{ \left| \int_{\mathcal{S}} \left(P'(s|\bar{s}, \bar{a}) - P(s|\bar{s}, \bar{a}) \right) f(s) ds \right\} \right\} : \|f\|_L \leq 1 \right\} \right. \\ \left. + L_{P^\pi} \sup_f \left\{ \left| \int_{\mathcal{S}} \left(d_{\pi,t-1}^{\mathcal{M}'}(\bar{s}) - d_{\pi,t-1}^{\mathcal{M}}(\bar{s}) \right) \frac{h_f(\bar{s})}{L_{P^\pi}} d\bar{s} \right| : \|f\|_L \leq 1 \right\} \right\} \quad (17)$$

$$= \sup_{s \in \mathcal{S}, a \in \mathcal{A}} d_{W_1}(P'(\cdot|s, a), P(\cdot|s, a)) + L_{P^\pi} d_{W_1}(d_{\pi,t-1}^{\mathcal{M}'}, d_{\pi,t-1}^{\mathcal{M}}), \quad (18)$$

where we plugged the common temporal relation $d_{\pi,t}^{\mathcal{M}}(s') = \int_{\mathcal{S}} \int_{\mathcal{A}} d_{\pi,t-1}^{\mathcal{M}}(s) \pi(a|s) P(s'|s, a) ds da$ into (14), we sum and subtract $\int_{\mathcal{S}} \int_{\mathcal{A}} \int_{\mathcal{S}} d_{\pi,t-1}^{\mathcal{M}'}(\bar{s}) \pi(\bar{a}|\bar{s}) P(s|\bar{s}, \bar{a}) ds d\bar{a} d\bar{s}$ to get (15), (16), and we apply the inequality in (12) to obtain (17) and then (18). To get rid of the dependence to the state distributions $d_{\pi,t-1}^{\mathcal{M}'}$ and $d_{\pi,t-1}^{\mathcal{M}}$, we repeatedly unroll (18) to get

$$d_{W_1}(d_{\pi,t}^{\mathcal{M}'}, d_{\pi,t}^{\mathcal{M}}) \leq \left(\sum_{j=0}^t L_{P^\pi}^j \right) \sup_{s \in \mathcal{S}, a \in \mathcal{A}} d_{W_1}(P'(\cdot|s, a), P(\cdot|s, a)) + L_{P^\pi}^t d_{W_1}(D', D) \quad (19)$$

$$= \left(\frac{1 - L_{P^\pi}^t}{1 - L_{P^\pi}} \right) \sup_{s \in \mathcal{S}, a \in \mathcal{A}} d_{W_1}(P'(\cdot|s, a), P(\cdot|s, a)) + L_{P^\pi}^t d_{W_1}(D', D), \quad (20)$$

where we note that $d_{W_1}(d_{\pi,0}^{\mathcal{M}'}, d_{\pi,0}^{\mathcal{M}}) = d_{W_1}(D', D)$ to derive (19), and we assume $L_{P^\pi} < 1$ (Assumption 1) to get (20) from (19). As a side note, when the state and action spaces are discrete, a natural choice of a metric is $d_S(s', s) = \mathbb{1}(s' \neq s)$ and $d_A(a', a) = \mathbb{1}(a' \neq a)$, which results in the Wasserstein distance being equivalent to the total variation, the constant $L_{P^\pi} = 1$, and $\sum_{j=0}^t L_{P^\pi}^j = t$. More details over the Lipschitz constant L_{P^π} can be found in (Pirotta, Restelli, and Bascetta 2015). Finally, we

can exploit the result in (20) to write

$$d_{W_1}(d_{\pi}^{\mathcal{M}'}, d_{\pi}^{\mathcal{M}}) = \sup_f \left\{ \left| \int_{\mathcal{S}} \left(\frac{1}{T} \sum_{t=0}^{T-1} d_{\pi,t}^{\mathcal{M}'}(s) - \frac{1}{T} \sum_{t=0}^{T-1} d_{\pi,t}^{\mathcal{M}}(s) \right) f(s) ds \right| : \|f\|_L \leq 1 \right\} \quad (21)$$

$$\begin{aligned} &\leq \frac{1}{T} \sum_{t=0}^{T-1} \sup_f \left\{ \left| \int_{\mathcal{S}} \left(d_{\pi,t}^{\mathcal{M}'}(s) - d_{\pi,t}^{\mathcal{M}}(s) \right) f(s) ds \right| : \|f\|_L \leq 1 \right\} \\ &\leq \frac{1}{T} \sum_{t=0}^{T-1} \frac{1 - L_{P^{\pi}}^t}{1 - L_{P^{\pi}}} \sup_{s \in \mathcal{S}, a \in \mathcal{A}} d_{W_1}(P'(\cdot|s, a), P(\cdot|s, a)) + L_{P^{\pi}}^t d_{W_1}(D', D) \\ &\leq \frac{1 - L_{P^{\pi}}^T}{1 - L_{P^{\pi}}} \sup_{s \in \mathcal{S}, a \in \mathcal{A}} d_{W_1}(P'(\cdot|s, a), P(\cdot|s, a)) + L_{P^{\pi}}^T d_{W_1}(D', D), \end{aligned} \quad (22)$$

in which we use (13) to get (21). The result follows from (22) by assuming the initial state distribution D to be shared across all the CMPs in \mathcal{M} , and taking the supremum over $P', P \in \mathcal{M}$. \square

Theorem B.2. Let \mathcal{M} be a class of CMPs, let $\pi \in \Pi$ be a policy, and let $d_{\pi}^{\mathcal{M}}$ be the marginal state distribution over T steps induced by π in $\mathcal{M} \in \mathcal{M}$. We can upper bound the π -diameter $\mathcal{D}_{\mathcal{M}}(\pi)$ as

$$\mathcal{D}_{\mathcal{M}}(\pi) := \sup_{\mathcal{M}', \mathcal{M} \in \mathcal{M}} d_{TV}(d_{\pi}^{\mathcal{M}'}, d_{\pi}^{\mathcal{M}}) \leq \sup_{P', P \in \mathcal{M}} T \mathbb{E}_{\substack{s \sim d_{\pi}^{\mathcal{M}} \\ a \sim \pi(\cdot|s)}} d_{TV}(P'(\cdot|s, a), P(\cdot|s, a)).$$

Proof. The proof follows techniques from (Metelli, Mutti, and Restelli 2018), especially Proposition 3.1. Without loss of generality, we take $\mathcal{M}', \mathcal{M} \in \mathcal{M}$. With some overloading of notation, we will alternatively identify a CMP with the tuple \mathcal{M} or its transition model P . Let us start considering the TV between the marginal state distributions induced by π over $\mathcal{M}', \mathcal{M}$, we can write

$$\begin{aligned} d_{TV}(d_{\pi}^{\mathcal{M}'}, d_{\pi}^{\mathcal{M}}) &= \frac{1}{2} \int_{\mathcal{S}} |d_{\pi}^{\mathcal{M}'}(s) - d_{\pi}^{\mathcal{M}}(s)| ds = \frac{1}{2} \int_{\mathcal{S}} \left| \frac{1}{T} \sum_{t=0}^{T-1} d_{\pi,t}^{\mathcal{M}'}(s) - \frac{1}{T} \sum_{t=0}^{T-1} d_{\pi,t}^{\mathcal{M}}(s) \right| ds \end{aligned} \quad (23)$$

$$\leq \frac{1}{2T} \sum_{t=0}^{T-1} \int_{\mathcal{S}} |d_{\pi,t}^{\mathcal{M}'}(s) - d_{\pi,t}^{\mathcal{M}}(s)| ds = \frac{1}{T} \sum_{t=0}^{T-1} d_{TV}(d_{\pi,t}^{\mathcal{M}'}, d_{\pi,t}^{\mathcal{M}}), \quad (24)$$

where we use (13) to get (23). Then, we provide an upper bound to each term of the final sum in (24), i.e.,

$$\begin{aligned} d_{TV}(d_{\pi,t}^{\mathcal{M}'}, d_{\pi,t}^{\mathcal{M}}) &= \frac{1}{2} \int_{\mathcal{S}} |d_{\pi,t}^{\mathcal{M}'}(s) - d_{\pi,t}^{\mathcal{M}}(s)| ds \\ &= \frac{1}{2} \int_{\mathcal{S}} \left| \int_{\mathcal{A}} \int_{\mathcal{S}} d_{\pi,t-1}^{\mathcal{M}'}(\bar{s}) \pi(\bar{a}|\bar{s}) P'(s|\bar{s}, \bar{a}) - d_{\pi,t-1}^{\mathcal{M}}(\bar{s}) \pi(\bar{a}|\bar{s}) P(s|\bar{s}, \bar{a}) \right| d\bar{s} d\bar{a} ds \end{aligned} \quad (25)$$

$$\leq \frac{1}{2} \int_{\mathcal{S}} |d_{\pi,t-1}^{\mathcal{M}'}(\bar{s}) - d_{\pi,t-1}^{\mathcal{M}}(\bar{s})| \int_{\mathcal{A}} \int_{\mathcal{S}} \pi(\bar{a}|\bar{s}) P'(s|\bar{s}, \bar{a}) d\bar{s} d\bar{a} ds \quad (26)$$

$$+ \frac{1}{2} \int_{\mathcal{S}} \int_{\mathcal{A}} d_{\pi,t-1}^{\mathcal{M}}(\bar{s}) \pi(\bar{a}|\bar{s}) \int_{\mathcal{S}} |P'(s|\bar{s}, \bar{a}) - P(s|\bar{s}, \bar{a})| d\bar{s} d\bar{a} ds \quad (27)$$

$$= d_{TV}(d_{\pi,t-1}^{\mathcal{M}'}, d_{\pi,t-1}^{\mathcal{M}}) + \mathbb{E}_{\substack{s \sim d_{\pi,t-1}^{\mathcal{M}} \\ a \sim \pi(\cdot|s)}} \left[d_{TV}(P'(\cdot|s, a), P(\cdot|s, a)) \right] \quad (28)$$

$$= \sum_{j=1}^{t-1} \mathbb{E}_{\substack{s \sim d_{\pi,j}^{\mathcal{M}} \\ a \sim \pi(\cdot|s)}} \left[d_{TV}(P'(\cdot|s, a), P(\cdot|s, a)) \right] + d_{TV}(D', D), \quad (29)$$

where we use the temporal relation $d_{\pi,t}^{\mathcal{M}}(s') = \int_{\mathcal{S}} \int_{\mathcal{A}} d_{\pi,t-1}^{\mathcal{M}}(s) \pi(a|s) P(s'|s, a) ds da$ to get (25), in which we sum and subtract $\int_{\mathcal{S}} \int_{\mathcal{A}} \int_{\mathcal{S}} d_{\pi,t-1}^{\mathcal{M}}(\bar{s}) \pi(\bar{a}|\bar{s}) P(s|\bar{s}, \bar{a}) ds d\bar{a} d\bar{s}$ to obtain (26) and (27), and we repeatedly unroll (28) to write (29), noting that

$d_{TV}(d_{\pi,0}^{\mathcal{M}'}, d_{\pi,0}^{\mathcal{M}}) = d_{TV}(D', D)$. Finally, we can plug (29) in (24) to get

$$\begin{aligned}
& d_{TV}(d_{\pi}^{\mathcal{M}'}, d_{\pi}^{\mathcal{M}}) \\
& \leq \frac{1}{T} \sum_{t=0}^{T-1} d_{TV}(d_{\pi,t}^{\mathcal{M}'}, d_{\pi,t}^{\mathcal{M}}) \\
& \leq \frac{1}{T} \sum_{t=0}^{T-1} \sum_{j=1}^{t-1} \mathbb{E}_{\substack{s \sim d_{\pi,j}^{\mathcal{M}} \\ a \sim \pi(\cdot|s)}} \left[d_{TV}(P'(\cdot|s, a), P(\cdot|s, a)) \right] + d_{TV}(D', D) \\
& \leq \sum_{t=0}^{T-1} \int_{\mathcal{S}} \frac{1}{T} \sum_{j=0}^{T-1} d_{\pi,j}^{\mathcal{M}}(s) \mathbb{E}_{a \sim \pi(\cdot|s)} \left[d_{TV}(P'(\cdot|s, a), P(\cdot|s, a)) \right] ds + d_{TV}(D', D) \tag{30}
\end{aligned}$$

$$= \sum_{t=0}^{T-1} \mathbb{E}_{\substack{s \sim d_{\pi}^{\mathcal{M}} \\ a \sim \pi(\cdot|s)}} \left[d_{TV}(P'(\cdot|s, a), P(\cdot|s, a)) \right] + d_{TV}(D', D) \tag{31}$$

$$= T \mathbb{E}_{\substack{s \sim d_{\pi}^{\mathcal{M}} \\ a \sim \pi(\cdot|s)}} \left[d_{TV}(P'(\cdot|s, a), P(\cdot|s, a)) \right] + d_{TV}(D', D), \tag{32}$$

in which we have used (13) to obtain (31) from (30). The final result is straightforward from (31) by assuming the initial state distribution D to be shared across all the CMPs in \mathcal{M} , and taking the supremum over $P', P \in \mathcal{M}$. \square

Theorem B.3. Let \mathcal{M} be a class of CMPs, let $\pi \in \Pi$ be a policy and $\mathcal{D}_{\mathcal{M}}(\pi)$ the corresponding π -diameter of \mathcal{M} . Let $d_{\pi}^{\mathcal{M}}$ be the marginal state distribution over T steps induced by π in $\mathcal{M} \in \mathcal{M}$, and let $\sigma_{\mathcal{M}} \leq \sigma_{\mathcal{M}} := \inf_{s \in \mathcal{S}} d_{\pi}^{\mathcal{M}}(s), \forall \mathcal{M} \in \mathcal{M}$. We can upper bound the entropy gap of the policy π within the model class \mathcal{M} as

$$\sup_{\mathcal{M}', \mathcal{M} \in \mathcal{M}} |H(d_{\pi}^{\mathcal{M}'}) - H(d_{\pi}^{\mathcal{M}})| \leq (\mathcal{D}_{\mathcal{M}}(\pi))^2 / \sigma_{\mathcal{M}} + \mathcal{D}_{\mathcal{M}}(\pi) \log(1/\sigma_{\mathcal{M}})$$

Proof. Let us expand the entropy gap of the policy π as

$$\begin{aligned}
& \sup_{\mathcal{M}', \mathcal{M} \in \mathcal{M}} |H(d_{\pi}^{\mathcal{M}'}) - H(d_{\pi}^{\mathcal{M}})| \\
& = \sup_{\mathcal{M}', \mathcal{M} \in \mathcal{M}} \left\{ \left| - \int_{\mathcal{S}} d_{\pi}^{\mathcal{M}'}(s) \log d_{\pi}^{\mathcal{M}'}(s) ds + \int_{\mathcal{S}} d_{\pi}^{\mathcal{M}}(s) \log d_{\pi}^{\mathcal{M}}(s) ds \right| \right\} \tag{33}
\end{aligned}$$

$$\leq \sup_{\mathcal{M}', \mathcal{M} \in \mathcal{M}} \left\{ \left| \int_{\mathcal{S}} (d_{\pi}^{\mathcal{M}}(s) - d_{\pi}^{\mathcal{M}'}(s)) \log d_{\pi}^{\mathcal{M}}(s) ds \right| + \left| \int_{\mathcal{S}} d_{\pi}^{\mathcal{M}'}(s) (\log d_{\pi}^{\mathcal{M}'}(s) - \log d_{\pi}^{\mathcal{M}}(s)) ds \right| \right\} \tag{34}$$

$$\leq \sup_{\mathcal{M}', \mathcal{M} \in \mathcal{M}} \left\{ -\log \sigma_{\mathcal{M}} \int_{\mathcal{S}} |d_{\pi}^{\mathcal{M}'}(s) - d_{\pi}^{\mathcal{M}}(s)| ds + D_{KL}(d_{\pi}^{\mathcal{M}'} || d_{\pi}^{\mathcal{M}}) \right\} \tag{35}$$

$$\leq \sup_{\mathcal{M}', \mathcal{M} \in \mathcal{M}} \left\{ -\log \sigma_{\mathcal{M}} D_{TV}(d_{\pi}^{\mathcal{M}'}, d_{\pi}^{\mathcal{M}}) + (D_{TV}(d_{\pi}^{\mathcal{M}'}, d_{\pi}^{\mathcal{M}}))^2 / \sigma_{\mathcal{M}} \right\} \tag{36}$$

$$\leq (\mathcal{D}_{\mathcal{M}}(\pi))^2 / \sigma_{\mathcal{M}} - \mathcal{D}_{\mathcal{M}}(\pi) \log \sigma_{\mathcal{M}} \tag{37}$$

in which we sum and subtract $\int_{\mathcal{S}} d_{\pi}^{\mathcal{M}'}(s) \log d_{\pi}^{\mathcal{M}}(s) ds$ to obtain (34) from (33), $\log d_{\pi}^{\mathcal{M}}(s)$ is upper bounded with $\log \sigma_{\mathcal{M}}$ to get (35), and we use the reverse Pinsker's inequality $D_{KL}(p||q) \leq (D_{TV}(p, q))^2 / \inf_{x \in \mathcal{X}} q(x)$ (Csiszár and Talata 2006, p. 1012 and Lemma 6.3) to obtain (10). Finally, we get the result by upper bounding $D_{TV}(d_{\pi}^{\mathcal{M}'}, d_{\pi}^{\mathcal{M}})$ with the π -diameter $\mathcal{D}_{\mathcal{M}}(\pi)$ and $\sigma_{\mathcal{M}}$ with $\sigma_{\mathcal{M}}$ in (36). \square

D Algorithm

In this section, we provide additional details about α MEPOL. A full implementation of the algorithm can be found at <https://github.com/muttimirco/alphamepol>.

D.1 The Benefits of the Baseline

In this section, we provide theoretical and empirical motivations to corroborate the use of the baseline $b = -\text{VaR}_{\alpha}(H_{\tau})$ into the Monte Carlo policy gradient estimator (Section 5, Equation 5). Thus, we compare the properties of two alternatives policy

gradient estimator, with and without a baseline, i.e.,

$$\begin{aligned}\widehat{\nabla}_{\theta} \mathcal{E}_{\mathcal{M}}^{\alpha}(\pi_{\theta}) &= \frac{1}{\alpha N} \sum_{i=1}^N f_{\tau_i} (\widehat{H}_{\tau_i} - \widehat{\text{VaR}}_{\alpha}(H_{\tau_i})) \mathbb{1}(\widehat{H}_{\tau_i} \leq \widehat{\text{VaR}}_{\alpha}(H_{\tau})), \\ \widehat{\nabla}_{\theta}^b \mathcal{E}_{\mathcal{M}}^{\alpha}(\pi_{\theta}) &= \frac{1}{\alpha N} \sum_{i=1}^N f_{\tau_i} (\widehat{H}_{\tau_i} - \text{VaR}_{\alpha}(H_{\tau_i}) - b) \mathbb{1}(\widehat{H}_{\tau_i} \leq \widehat{\text{VaR}}_{\alpha}(H_{\tau})).\end{aligned}$$

where $f_{\tau_i} = \sum_{t=0}^{T-1} \nabla_{\theta} \log \pi_{\theta}(a_{t,\tau_i} | s_{t,\tau_i})$. The former ($\widehat{\nabla}_{\theta} \mathcal{E}_{\mathcal{M}}^{\alpha}$) is known to be asymptotically unbiased (Tamar, Glassner, and Mannor 2015), but it is hampered by the estimation error of the VaR term to be subtracted to each \widehat{H}_{τ_i} in finite sample regimes (Kolla et al. 2019). The latter ($\widehat{\nabla}_{\theta}^b \mathcal{E}_{\mathcal{M}}^{\alpha}$) introduces some bias in the estimate, but it crucially avoids the estimation error of the VaR term to be subtracted, as it cancels out with the baseline b . The following proposition, along with related lemmas, assesses the critical number of samples (n^*) for which an upper bound to the bias of $\widehat{\nabla}_{\theta}^b \mathcal{E}_{\mathcal{M}}^{\alpha}$ is lower to the estimation error of $\widehat{\nabla}_{\theta} \mathcal{E}_{\mathcal{M}}^{\alpha}$.

Lemma D.1. *The expected bias of the policy gradient estimate $\widehat{\nabla}_{\theta}^b \mathcal{E}_{\mathcal{M}}^{\alpha}(\pi_{\theta})$ can be upper bounded as*

$$\mathbb{E}_{\substack{\mathcal{M} \sim \mathcal{M} \\ \tau_i \sim p_{\pi_{\theta}, \mathcal{M}}}} [\text{bias}] = \mathbb{E}_{\substack{\mathcal{M}_i \sim \mathcal{M} \\ \tau_i \sim p_{\pi_{\theta}, \mathcal{M}_i}}} [\nabla_{\theta} \mathcal{E}_{\mathcal{M}}^{\alpha}(\pi_{\theta}) - \widehat{\nabla}_{\theta}^b \mathcal{E}_{\mathcal{M}}^{\alpha}(\pi_{\theta})] \leq \mathcal{U} \alpha b,$$

where \mathcal{U} is a constant such that $f_{\tau_i} \leq \mathcal{U}$ for all τ_i .

Proof. This Lemma can be easily derived by means of

$$\begin{aligned}& \mathbb{E}_{\substack{\mathcal{M}_i \sim \mathcal{M} \\ \tau_i \sim p_{\pi_{\theta}, \mathcal{M}_i}}} [\text{bias}] \\&= \mathbb{E}_{\substack{\mathcal{M}_i \sim \mathcal{M} \\ \tau_i \sim p_{\pi_{\theta}, \mathcal{M}_i}}} \left[\nabla_{\theta} \mathcal{E}_{\mathcal{M}}^{\alpha}(\pi_{\theta}) - \widehat{\nabla}_{\theta}^b \mathcal{E}_{\mathcal{M}}^{\alpha}(\pi_{\theta}) \right] \\&= \nabla_{\theta} \mathcal{E}_{\mathcal{M}}^{\alpha}(\pi_{\theta}) - \mathbb{E}_{\substack{\mathcal{M}_i \sim \mathcal{M} \\ \tau_i \sim p_{\pi_{\theta}, \mathcal{M}_i}}} \left[\frac{1}{\alpha N} \sum_{i=1}^N f_{\tau_i} (\widehat{H}_{\tau_i} - \text{VaR}_{\alpha}(H_{\tau_i}) - b) \mathbb{1}(\widehat{H}_{\tau_i} \leq \widehat{\text{VaR}}_{\alpha}(H_{\tau})) \right] \\&= \nabla_{\theta} \mathcal{E}_{\mathcal{M}}^{\alpha}(\pi_{\theta}) - \mathbb{E}_{\substack{\mathcal{M} \sim \mathcal{M} \\ \tau \sim p_{\pi_{\theta}, \mathcal{M}}}} \left[f_{\tau} (\widehat{H}_{\tau} - \text{VaR}_{\alpha}(H_{\tau}) - b) \mathbb{1}(\widehat{H}_{\tau} \leq \widehat{\text{VaR}}_{\alpha}(H_{\tau})) \right] \tag{38}\end{aligned}$$

$$= \nabla_{\theta} \mathcal{E}_{\mathcal{M}}^{\alpha}(\pi_{\theta}) - \nabla_{\theta} \mathcal{E}_{\mathcal{M}}^{\alpha}(\pi_{\theta}) + \mathbb{E}_{\substack{\mathcal{M} \sim \mathcal{M} \\ \tau \sim p_{\pi_{\theta}, \mathcal{M}}}} \left[f_{\tau} b \mathbb{1}(\widehat{H}_{\tau} \leq \widehat{\text{VaR}}_{\alpha}(H_{\tau})) \right] \tag{39}$$

$$= \mathbb{E}_{\substack{\mathcal{M} \sim \mathcal{M} \\ \tau \sim p_{\pi_{\theta}, \mathcal{M}}}} \left[f_{\tau} b \mathbb{1}(\widehat{H}_{\tau} \leq \widehat{\text{VaR}}_{\alpha}(H_{\tau})) \right] \leq \mathcal{U} \alpha b, \tag{40}$$

where (39) follows from (38) by noting that the estimator without the baseline term is unbiased (Tamar, Glassner, and Mannor 2015), and (40) is obtained by upper bounding f_{τ} with \mathcal{U} and noting that $\mathbb{E}_{\substack{\mathcal{M} \sim \mathcal{M} \\ \tau \sim p_{\pi_{\theta}, \mathcal{M}}}} [\mathbb{1}(\widehat{H}_{\tau} \leq \widehat{\text{VaR}}_{\alpha}(H_{\tau}))] = \alpha$. \square

Lemma D.2 (VaR concentration bound from (L.A., Jagannathan, and Kolla 2020)). *Let X be a continuous random variable with a pdf f_X for which there exist $\eta, \Delta > 0$ such that $f_X(x) > \eta$ for all $x \in [\text{VaR}_{\alpha}(X) - \frac{\Delta}{2}, \text{VaR}_{\alpha}(X) + \frac{\Delta}{2}]$. Then, for any $\epsilon > 0$ we have*

$$\Pr[|\widehat{\text{VaR}}_{\alpha}(X)_{\alpha} - \text{VaR}_{\alpha}(X)| \geq \epsilon] \leq 2 \exp(-2n\eta^2 \min(\epsilon^2, \Delta^2)),$$

where $n \in \mathbb{N}$ is the number of samples employed to estimate $\widehat{\text{VaR}}_{\alpha}(X)$.

Proposition D.3. *Let $\widehat{\nabla}_{\theta} \mathcal{E}_{\mathcal{M}}^{\alpha}(\pi_{\theta})$ and $\widehat{\nabla}_{\theta}^b \mathcal{E}_{\mathcal{M}}^{\alpha}(\pi_{\theta})$ be policy gradient estimates with and without a baseline. Let f_H be the pdf of H_{τ} , for which there exist $\eta, \Delta > 0$ such that $f_H(H_{\tau}) > \eta$ for all $H_{\tau} \in [\text{VaR}_{\alpha}(H_{\tau}) - \frac{\Delta}{2}, \text{VaR}_{\alpha}(H_{\tau}) + \frac{\Delta}{2}]$. The number of samples n^* for which the estimation error ϵ of $\widehat{\nabla}_{\theta} \mathcal{E}_{\mathcal{M}}^{\alpha}(\pi_{\theta})$ is lower than the bias of $\widehat{\nabla}_{\theta}^b \mathcal{E}_{\mathcal{M}}^{\alpha}(\pi_{\theta})$ with at least probability $\delta \in (0, 1)$ is given by*

$$n^* = \frac{\log 2/\delta}{2\eta^2 \min(\mathcal{U}^2 \alpha^2 b^2, \Delta^2)}.$$

Proof. The proof is straightforward by considering the estimation error ϵ of $\widehat{\nabla}_{\theta} \mathcal{E}_{\mathcal{M}}^{\alpha}(\pi_{\theta})$ equal to the upper bound of the bias of $\widehat{\nabla}_{\theta}^b \mathcal{E}_{\mathcal{M}}^{\alpha}(\pi_{\theta})$ from Lemma D.1, i.e., $\epsilon = \mathcal{U}\alpha b$. Then, we set $\delta = 2 \exp(-2n^* \eta^2 \min(\mathcal{U}^2 \alpha^2 b^2, \Delta^2))$ from Lemma D.2, which gives the result through simple calculations. \square

The Proposition D.3 proves that there is little incentive to choose the policy gradient estimator $\widehat{\nabla}_{\theta} \mathcal{E}_{\mathcal{M}}^{\alpha}$ when the number of trajectories is lower than n^* , as its estimation error would exceed the bias introduced by the alternative estimator $\widehat{\nabla}_{\theta}^b \mathcal{E}_{\mathcal{M}}^{\alpha}$. Unfortunately, it is not easy to compute n^* in our setting, as we do not assume to know the distribution of H_{τ} , but the requirement is arguably seldom matched in practice.

Moreover, we can empirically show that the baseline $b = -\text{VaR}_{\alpha}(H_{\tau})$ might benefit the variance of the policy gradient estimation, at the expense of the additional bias which is anyway lower than the estimation error of $\widehat{\nabla}_{\theta} \mathcal{E}_{\mathcal{M}}^{\alpha}$. In Figure 6 (left), we can see that the exploration performance $\mathcal{E}_{\mathcal{M}}^{\alpha}$ obtained by α MEPOL with and without the baseline is essentially the same in the illustrative *GridWorld with Slope* domain. Whereas Figure 6 (right) suggests a slightly inferior variance for the policy gradient estimate employed by α MEPOL with the baseline.

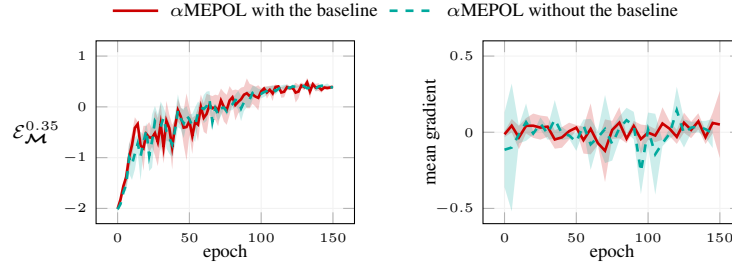


Figure 6: Comparison of the exploration performance $\mathcal{E}_{\mathcal{M}}^{0.35}$ (left) and sampled gradients of the policy mean (right) achieved by α MEPOL ($\alpha = 0.35$) with and without the baseline $b = -\text{VaR}_{\alpha}(H_{\tau})$ in the policy gradient estimation (5). We provide 95% c.i. over 4 runs.

D.2 Importance Weighted Entropy Estimation

As done in (Mutti, Pratissoli, and Restelli 2021), we build on the estimator in (3) to consider the case in which the target policy $\pi_{\theta'}$ differs from the sampling policy π_{θ} . The idea is to combine two successful policy-search methods. The first one is POIS (Metelli et al. 2018), to perform the optimization offline via importance sampling, allowing for an efficient exploitation of the samples collected with previous policies. We thus adopt an Importance-Weighted (IW) entropy estimator (Ajgl and Šimandl 2011) of the form

$$\widehat{H}_{\tau_i}^{\text{IW}} = - \sum_{t=0}^{T-1} \frac{\sum_{j \in \mathcal{N}_t^k} w_j}{k} \ln \frac{\Gamma(\frac{p}{2} + 1) \sum_{j \in \mathcal{N}_t^k} w_j}{\|s_{t,\tau_i} - s_{t,\tau_i}^{k\text{-NN}}\|^p \pi^{\frac{p}{2}}} + \ln k - \Psi(k), \quad (41)$$

where $\ln k - \Psi(k)$ is a bias correction term in which Ψ is the Digamma function, \mathcal{N}_t^k is the set of indices of the k -NN of s_{t,τ_i} , and w_j are the normalized importance weights of samples s_{j,τ_i} . To compute these importance weights we consider a dataset $\mathcal{D} = \{s_{t,\tau_i}\}_{t=0}^{T-1}$ by looking each state encountered in a trajectory as an unweighted particle. Then, we expand it as $\mathcal{D}_{\tau_i} = \{(\tau_{i,t}, s_t)\}_{t=0}^{T-1}$, where $\tau_{i,t} = (s_{0,\tau_i}, \dots, s_{t,\tau_i})$ is the portion of the trajectory that leads to state s_{t,τ_i} . This allows to associate each particle s_{t,τ_i} to its importance weight \widehat{w}_t and normalized importance weight w_t for any pair of target ($\pi_{\theta'}$) and sampling (π_{θ}) policies:

$$\widehat{w}_t = \frac{p(\tau_{i,t}|\pi_{\theta'})}{p(\tau_{i,t}|\pi_{\theta})} = \prod_{z=0}^t \frac{\pi_{\theta'}(a_{z,\tau_i}|s_{z,\tau_i})}{\pi_{\theta}(a_{z,\tau_i}|s_{z,\tau_i})}, \quad w_t = \frac{\widehat{w}_t}{\sum_{n=0}^{T-1} \widehat{w}_n}.$$

The estimator in (41) is then optimized via gradient ascent within a trust-region around the current policy. The trust-region constraint is obtained by imposing

$$\widehat{D}_{KL}(\pi_{\theta'}||\pi_{\theta}) = \frac{1}{T} \sum_{t=0}^{T-1} \ln \frac{k/T}{\sum_{j \in \mathcal{N}_t^k} w_j} \leq \delta,$$

where $\widehat{D}_{KL}(\pi_{\theta'}||\pi_{\theta})$ is a non-parametric IW k -NN estimate of the Kullback-Leibler (KL) divergence (Ajgl and Šimandl 2011). Its value is computed as in (Mutti, Pratissoli, and Restelli 2021), by considering the entire batch of trajectories collected to execute the off-policy optimization steps as a single trajectory.

Algorithm 2: α MEPOL

Input: initial policy π_{θ_0} , exploration horizon T , number of trajectories N , batch-size B , percentile α , learning rate β , trust-region threshold δ , sampling distribution $p_{\mathcal{M}}$

Output: exploration policy π_{θ_h}

```
1: for epoch = 0, 1, ..., until convergence do
2:   for  $i = 1, 2, \dots, N$  do
3:     sample an environment  $\mathcal{M}_i \sim p_{\mathcal{M}}$ 
4:     for  $j = 1, 2, \dots, B$  do
5:       sample a trajectory  $\tau_j \sim p_{\pi_{\theta}, \mathcal{M}_i}$  of length  $T$ 
6:     end for
7:   end for
8:   initialize dataset  $\mathcal{D} = \emptyset$ , off-policy step  $h = 0$  and  $\theta_h = \theta$ 
9:   while  $\widehat{D}_{KL}(\pi_{\theta_0} || \pi_{\theta_h}) \leq \delta$  do
10:    for  $j = 1, 2, \dots, B$  do
11:      estimate  $H_{\tau_j}$  with (41)
12:      append  $\widehat{H}_{\tau_j}$  to  $\mathcal{D}$ 
13:    end for
14:    sort  $\mathcal{D}$  and split it in  $\mathcal{D}_{\alpha}$  and  $\mathcal{D}_{1-\alpha}$ 
15:    compute a gradient step  $\theta_{h+1} = \theta_h + \beta \widehat{\nabla}_{\theta_h} \mathcal{E}_{\mathcal{M}}^{\alpha}(\pi_{\theta_h})$ 
16:     $h \leftarrow h + 1$ 
17:  end while
18:   $\theta \leftarrow \theta_h$ 
19: end for
```

D.3 Algorithmic Details of α MEPOL

In this section, we provide an extended pseudocode (Algorithm 2) of α MEPOL, along with some additional comments.

Given a probability distribution $p_{\mathcal{M}}$, the algorithm operates by iteratively sampling an environment $\mathcal{M}_i \in \mathcal{M}$ drawn according to $p_{\mathcal{M}}$ and then sampling B trajectories of length T from it using π_{θ} , where B is the dimension of each mini-batch. Then, the estimate of the entropy of each mini-batch \widehat{H}_{τ_j} is computed by means of the estimator in (41) and appended to the dataset \mathcal{D} . Once the dataset \mathcal{D} is obtained, we can straightforwardly derive a risk-sensitive policy update by just subsampling from it, so that to keep only the realizations below the α -percentile. This can be easily done by sorting \mathcal{D} in ascending order and considering only the αN first mini-batches. Then, we can compute the gradient as follows:

$$\widehat{\nabla}_{\theta} \mathcal{E}_{\mathcal{M}}^{\alpha}(\pi_{\theta}) = \frac{1}{\alpha N} \sum_{i=1}^N f_{\tau_i} \widehat{H}_{\tau_i} \mathbb{1}(\widehat{H}_{\tau_i} \leq \widehat{\text{VaR}}_{\alpha}(H_{\tau})).$$

The operations carried out once all the trajectories have been sampled are executed in a fully off-policy manner, in which we repeat the same steps until the trust-region boundary is reached or until the number of off-policy iterations exceeds a specified limit. The reason why we introduce an additional parameter B , instead of considering one trajectory at a time, is due to the fact that a significant amount of samples (see the parameters in Table 1) is needed to obtain a reliable estimate of the entropy, noting that the entropy estimator is only asymptotically unbiased.

E Experiments

In this section, we report an extensive description of the conducted experiments, with the corresponding hyperparameter values and some additional plots and experiments.

E.1 Environments

We use three different environments in our experiments. The first one is a custom implementation of a gridworld, coded from scratch. The second one is an adapted version of the rllab Ant-Maze environment (Duan et al. 2016).

GridWorld with Slope In *GridWorld with Slope* (2D states, 2D actions), the agent can move inside a map composed of four rooms connected by four narrow hallways, by choosing at each step how much to move on the x and y axes. The side of the environment measures 2 units and the maximum viable space of the agent at each step is 0.2. Thus, the agent needs around 10 steps to go from one side to the other on a straight line. When the agent collides with the external borders or with the internal walls, it is re-positioned according to a custom function. This is done not only to make the interaction more realistic, but also to limit the possibility to have a negative infinite entropy resulting from the k-NN computation, which can occur when the samples

are too close and the value of the parameter k is not high enough. This precaution is particularly useful in our scenario, due to the presence of a slope, and especially in the *adversarial* configuration GWN, because of the initial position of the agent, which is sampled in a small square in the top-right corner. It is easy to see that in the first epochs in the GWN environment, the agent would repeatedly collide with the top-border, leading in general to a much more lower entropy w.r.t. to GWS.

The slope is applied only in the upper half of the environment, since we found this to be a good trade-off between the intention of maintaining a difference in terms of risk among the two configurations and the overall complexity of the exploration. Indeed, we noted that by applying the slope to the whole GridWorld, the advantage in terms of exploration entailed by the risk-averse approach is even higher, but it struggles to explore the bottom states of the environment with a reasonable number of samples. The slope is computed as $s \sim \mathcal{N}(\frac{\Delta_{max}}{2}, \frac{\Delta_{max}}{20})$, where $\Delta_{max} = 0.2$ is the maximum step that the agent can perform.

MultiGrid In *MultiGrid*, everything works as in *GridWorld with Slope*, but we indeed have 10 configurations. These environments differ for both the shape and the type of slope to which they are subject to. The *adversarial* configuration is still GWN, but the slope is computed as $s \sim \mathcal{N}(\frac{\Delta_{max}}{2.6}, \frac{\Delta_{max}}{20})$, where $\Delta_{max} = 0.2$. The other 9 gridworlds have instead a different arrangement of the walls (see the heatmaps in Figure 10) and the slope, computed as $s \sim \mathcal{N}(\frac{\Delta_{max}}{3.2}, \frac{\Delta_{max}}{20})$ with $\Delta_{max} = 0.2$, is applied over the entire environment. Two configurations are subject to south-facing slope, three to east-facing slope, one to south-east-facing slope and three to no slope at all.

Ant Stairs We adopt the Ant-Maze environment (29D states, 8D actions) of rllab (Duan et al. 2016) and we exploit its malleability to build two custom configurations which could fit our purposes. The adverse configuration consists of a narrow ascending staircase (*Ant Stairs Up*) made up of an initial square (the initial position of the Ant), followed by three blocks of increasing height. The simpler configuration consists of a wide descending staircase (*Ant Stairs Down*), made up of 3×3 blocks of decreasing height and a final 1×3 flat area. Each block has a side length slightly greater than the Ant size. A visual representation of such settings is provided in Figure 11. During the *Unsupervised Pre-Training* phase, $\mathcal{E}_{\mathcal{M}}^{\alpha}$ is maximized over the x,y spatial coordinates of the ant’s torso.

MiniGrid We use the MiniGrid suite (Chevalier-Boisvert, Willems, and Pal 2018), which consists of a set of fast and light-weighted gridworld environments. The environments are partially observable, with the dimension of the agent’s field of view having size $7 \times 7 \times 3$. Both the observation space \mathcal{S} and the action space \mathcal{A} are discrete, and in each tile of the environment there can be only one object at the same time. The set of objects is $\mathcal{O} = \{wall, floor, lava, door, key, ball, box, goal\}$. The agent can move inside the grid and interact with these objects according to their properties. In particular, the actions comprise turning left, turning right, moving forward, picking up an object, dropping an object and toggling, i.e., interacting with the objects (e.g., to open a door). We exploit the suite’s malleability to build two custom environments. The simpler one has a size of 18×18 , and it simply contains some sparse walls. The adverse configuration is smaller, 10×10 , and is characterized by the presence of a door at the top of a narrow hallway. The door is closed but not locked, meaning that the agent can open it without using a key. Moreover, we modify the movement of the agent so that the direction is given by the bottom of the triangle instead of the top. The intuition is that by doing this we are essentially changing the shape of the agent, causing an additional hurdle for the exploration.

As regards the training procedure, everything remains the same, except for two differences. The first difference is that the k -NN computation is performed on the representation space generated by a fixed random encoder. Note that this random encoder is not part of the policy. It is randomly initialized and not updated during the training in order to produce a more stable entropy estimate. In addition, before computing the distances, we apply to its output a random Gaussian noise $\epsilon \sim \mathcal{N}(0.001, 0.001)$ truncated in $[0, 0.001]$. We do this to avoid the aliasing problem, which occurs when we have many samples (more than k) in the same position, thus having zero distance and producing a negative infinite entropy estimate. The homogeneity of the MiniGrid environments in terms of features make this problem more frequent. The second difference is the addition of a bootstrapping procedure for the easy configuration, meaning that we use only a subset of the mini-batches of the easy configuration to update the policy. Especially, we randomly sample a number of mini-batches that is equal to the dimension of the \mathcal{D}_{α} dataset so that MEPOL uses the same number of samples of α MEPOL. The reason why we avail this method is to avoid a clear advantage for MEPOL in learning effective representations, since it usually access more samples than α MEPOL. Note that it is not a stretch, since we are essentially balancing the information available to the two algorithms.

E.2 Class of Policies

In all the experiments but one the policy is a Gaussian distribution with diagonal covariance matrix. It takes as input the environment state features and outputs an action vector $a \sim \mathcal{N}(\mu, \sigma^2)$. The mean μ is state-dependent and is the downstream output of a densely connected neural network. The standard deviation is state-independent and it is represented by a separated trainable vector. The dimension of μ , σ , and a vectors is equal to the action-space dimension of the environment. The only experiment with a different policy is the MiniGrid one, for which we adopt the architecture recently proposed by (Seo et al. 2021). Thus, we use a random encoder made up of 3 convolutional layers with kernel 2, stride 1, and padding 0, each activated by a ReLU function, and with 16, 32 and 64 filters respectively. The first ReLU is followed by a 2D max pooling layer with kernel 2. The output of the encoder is a 64 dimensional tensor, which is then fed to a feed-forward neural network with two fully-connected layers with hidden dimension 64 and a Tanh activation function.

E.3 Hyperparameter Values

To choose the values of the hyper-parameters of α MEPOL, MEPOL, and TRPO with the corresponding initialization, we mostly relied on the values reported in (Mutti, Pratisoli, and Restelli 2021, Appendix C.3, C.4), which have been optimized for a risk-neutral approach to the maximum state entropy setting (i.e., the MEPOL baseline). By avoiding to specifically fine-tune the hyper-parameters for the α MEPOL algorithm (and TRPO with α MEPOL initialization), we obtain conservative comparisons between α MEPOL and the MEPOL baseline.

Unsupervised Pre-Training In Table 1, we report the parameters of α MEPOL and MEPOL that are used in the experiments described in Section 6.1, Section 6.2, Section 6.4 and Section 6.5.

Table 1: α MEPOL and MEPOL Parameters for the Unsupervised Pre-Training

	GRIDWORLD WITH SLOPE	MULTIGRID	ANT	MINIGRID
NUMBER OF EPOCHS	150	50	400	300
HORIZON (T)	400	400	400	150
NUMBER OF TRAJ. (N)	200	500	150	100
MINI-BATCH DIMENSION (B)	5	5	5	5
α -PERCENTILE	0.2	0.1	0.2	0.2
SAMPLING DIST. ($p_{\mathcal{M}}$)	[0.8,0.2]	[0.1,...,0.1]	[0.8,0.2]	[0.8,0.2]
KL THRESHOLD (δ)	15	15	15	15
LEARNING RATE (β)	10^{-5}	10^{-5}	10^{-5}	10^{-5}
NUMBER OF NEIGHBORS (k)	30	30	500	50
POLICY HIDDEN LAYER SIZES	(300,300)	(300,300)	(400,300)	*
POLICY HIDDEN LAYER ACT. FUNCT.	ReLU	ReLU	ReLU	*
NUMBER OF SEEDS	10	10	10	10

* See Section E.2 for full details on the architecture.

Supervised Fine-Tuning In Table 2, we report the TRPO parameters that are used in the experiments described in Section 6.3, Section 6.4, Section 6.5 and Section 6.7.

Table 2: TRPO Parameters for the Supervised Fine-Tuning

	GRIDWORLD WITH SLOPE	MULTIGRID	ANT	MINIGRID
NUMBER OF ITER.	100	100	100	200
HORIZON	400	400	400	150
SIM. STEPS PER ITER.	1.2×10^4	1.2×10^4	4×10^4	7.5×10^3
δ_{KL}	10^{-4}	10^{-4}	10^{-2}	10^{-4}
DISCOUNT (γ)	0.99	0.99	0.99	0.99
NUMBER OF SEEDS	50	50	8	13
NUMBER OF GOALS	50	50	8	13

Meta-RL In Table 3 and Table 4, we report the MAML and DIAYN parameters that are used in the experiments described in Section 6.7, in order to meta-train a policy on the *GridWorld with Slope* and *MultiGrid* domains. For MAML, we adopted the codebase at <https://github.com/tristandeleu/pytorch-maml-rl>, while for DIAYN, we used the original implementation.

Table 3: MAML Parameters for the Meta-Training

	GRIDWORLD WITH SLOPE	MULTIGRID
NUMBER OF BATCHES	200	200
META BATCH SIZE	20	20
FAST BATCH SIZE	30	30
NUM. OF GRAD. STEP	1	1
HORIZON	400	400
FAST LEARNING RATE	0.1	0.1
POLICY HIDDEN LAYER SIZES	(300,300)	(300,300)
POLICY HIDDEN LAYER ACT. FUNCTION	RELU	RELU
NUMBER OF SEEDS	8	8

Table 4: DIAYN Parameters

	GRIDWORLD WITH SLOPE	MULTIGRID
NUMBER OF EPOCHS	1000	1000
HORIZON	400	400
NUMBER OF SKILLS	20	20
LEARNING RATE	3×10^{-4}	3×10^{-4}
DISCOUNT (γ)	0.99	0.99
POLICY HIDDEN LAYER SIZES	(300,300)	(300,300)
POLICY HIDDEN LAYER ACT. FUNCTION	RELU	RELU
NUMBER OF SEEDS	8	8

E.4 Counterexamples: When Percentile Sensitivity Does Not Matter

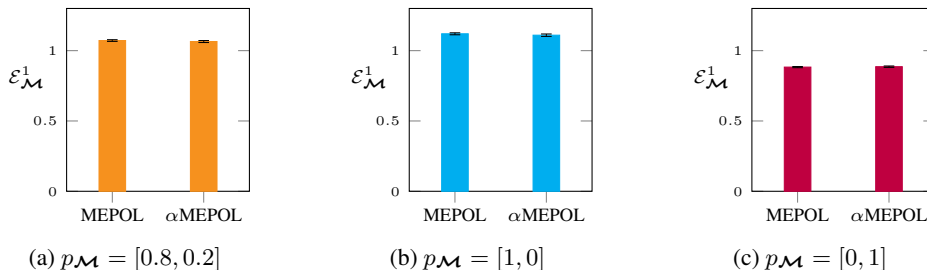


Figure 7: Comparison of the exploration performance $\mathcal{E}_{\mathcal{M}}^1$ obtained by α MEPOL ($\alpha = 0.35$) and MEPOL in the *GridWorld Counterexample* domain. The policies are trained (50 epochs, 8×10^4 samples per epoch) on the configuration (a) and tested on (a, b, c). We provide 95% c.i. over 4 runs.

In this section, we provide a couple of convenient example to confirm the fact that there are classes of environments in which we would not need any particularly smart solution for the multiple environments problem, beyond a naïve, risk-neutral approach. First, we consider two GridWorld environments that differ for the shape of the traversable area, sampled according to $p_{\mathcal{M}} = [0.8, 0.2]$, and we run α MEPOL with $\alpha = 0.35$ and MEPOL, obtaining the two corresponding exploration policies. In Figure 7 we show the performance (measured by $\mathcal{E}_{\mathcal{M}}^1$) obtained by executing those policies on each setting. Clearly, regardless of what configuration we consider, there is no advantage deriving from the use of a risk-averse approach as α MEPOL, meaning that the class of environments \mathcal{M} is balanced in terms of hardness of exploration.

In the second counterexample, we consider different configurations of the MiniGrid (Chevalier-Boisvert, Willems, and Pal 2018) domain that we considered in Section 6.6. Especially, we aim to show that configurations that are visibly different from an human perspective are sometimes not really challenging from a multiple environments standpoint. Indeed, this setting would be challenging only if the policy that the agent should deploy to explore one configuration is significantly different to the one needed to explore another configuration. In this case, the agent should trade-off the performance in one configuration and the other. As we show in Figure 8, the combination of Unlock-v0 and ObstructedMaze-2Dlhb-v0 does not have this feature, and the MEPOL baseline is able to find a policy that works well in both the configurations.

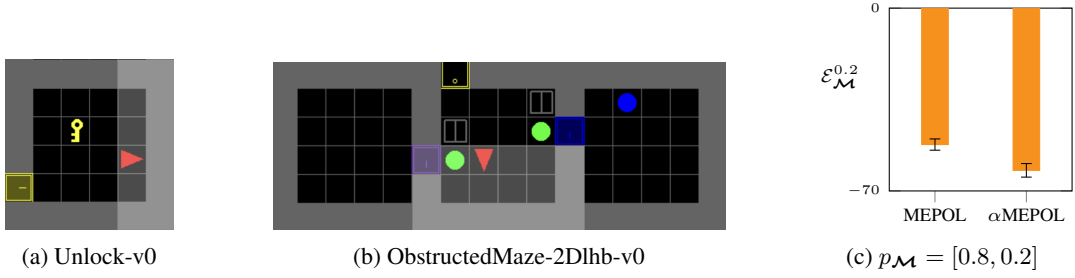


Figure 8: Comparison of the exploration performance $\mathcal{E}_{\mathcal{M}}^{0.2}$ obtained by α MEPOL ($\alpha = 0.2$) and MEPOL (c) in a *MiniGrid* domain with the configurations *Unlock-v0* (a) and *ObstructedMaze-2Dlhb-v0* (b). We provide 95% c.i. over 8 runs.

E.5 Further Details on Meta-RL Experiments

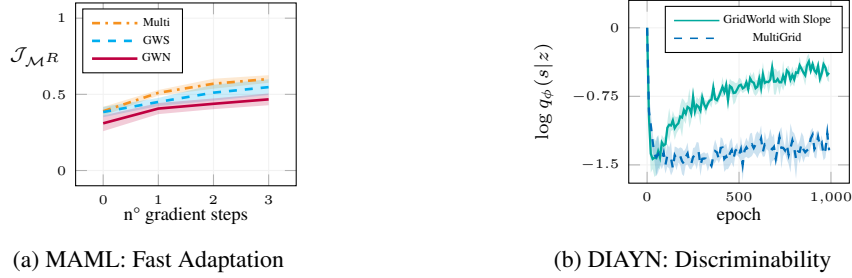


Figure 9: We illustrate the fast-adapting behavior of MAML in the *GridWorld with Slope* (a), and the skills discriminability of DIAYN as a function of learning epochs (b). We provide 95% c.i. over 8 runs.

In this section, we provide additional details on the experiments of Section 6.7. Especially, we show that MAML does perform well on its own objective, which is to learn a fast-adapting policy during meta-training (Figure 9a). Instead, in Figure 9b we highlight the performance measure of DIAYN (Eysenbach et al. 2018). In particular, the more $\log q_{\phi}(s|z)$ grows with the learning epochs, the better is the intrinsic reward we feed to MAML+DIAYN. Clearly, DIAYN struggles to deal with the larger *MultiGrid* class of environments, which explains the inferior performance of MAML+DIAYN in this domain.

E.6 Additional Visualizations

In this section, we provide some additional visualizations, which are useful to better understand some of the domains used in the experiments of Section 6. In Figure 10 we report the state-visitation frequencies achieved by α MEPOL (Figure 10a) and MEPOL (Figure 10b) in each configuration of the *MultiGrid* domain. Clearly, α MEPOL manages to obtain a better exploration in the adversarial configuration w.r.t. MEPOL, especially in the bottom part of the environment, which is indeed the most difficult part to visit. On the other environments, the performance is overall comparable. In Figure 11 we show a render of the *Ant Stairs* domain, illustrating both the environments used in the experiments of Section 6.5. Note that the front walls are hidden to allow for a better visualization.

F Future Directions

First, it is worth mentioning an alternative setting in which α MEPOL can be employed with benefit (with little or no modifications). This is the *robust unsupervised exploration* problem, in which we just have to replace the class of environments with a single CMP specified under uncertainty (Satia and Lave Jr 1973). Secondly, in this work we focused on a specific solution for an essentially multi-objective problem, by establishing a preference over the environments through the CVaR objective. Instead, a future direction could pursue learning a direct approximation of the Pareto frontier (Parisi, Pirota, and Restelli 2016) of the exploration strategies over multiple environments. Another promising direction is to assume some control over the class distribution during the unsupervised pre-training process, either by an external supervisor or by the agent itself (Metelli, Mutti, and Restelli 2018). Lastly, future work may establish regret guarantees for the reward-free exploration problem over multiple environments, in a similar flavor to the reward-free RL problem in a single environment (Jin et al. 2020).

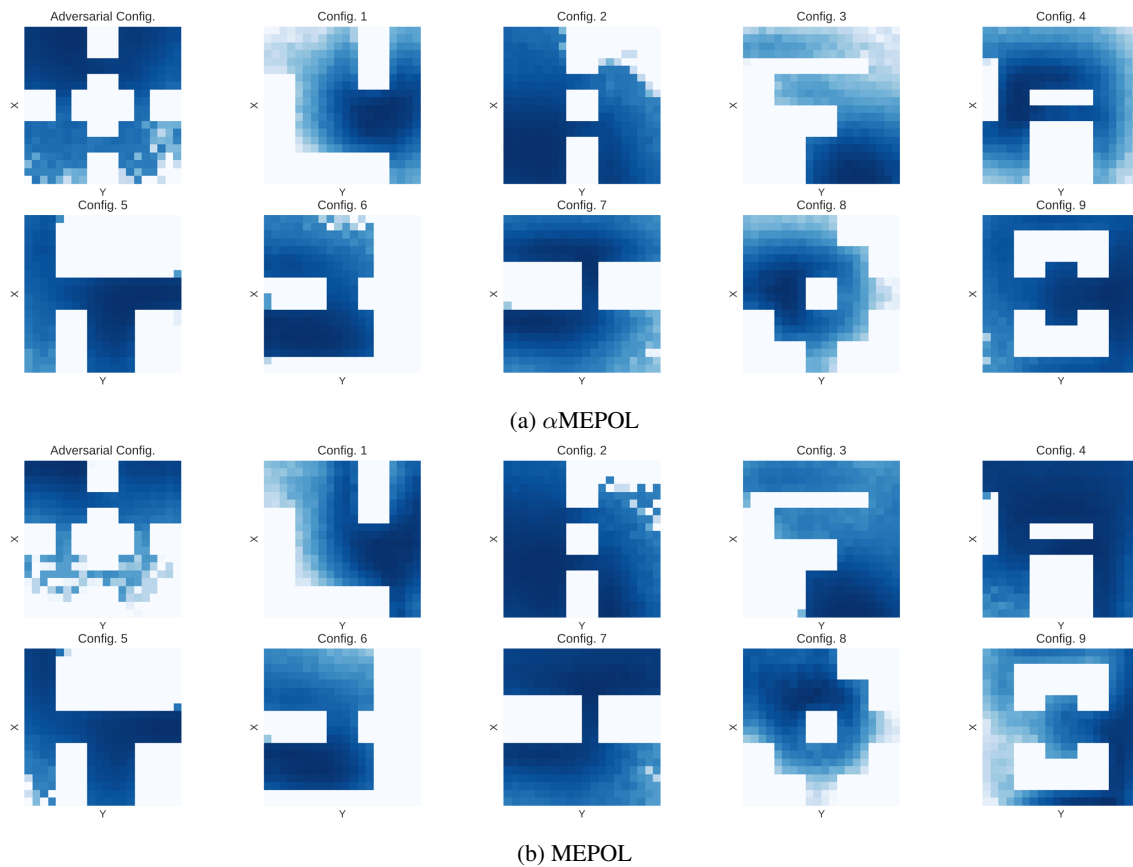


Figure 10: Heatmaps of the state visitations (200 trajectories) induced by the exploration policies trained with α MEPOL ($\alpha = 0.1$) **(a)** and MEPOL **(b)** in the *MultiGrid* domain.

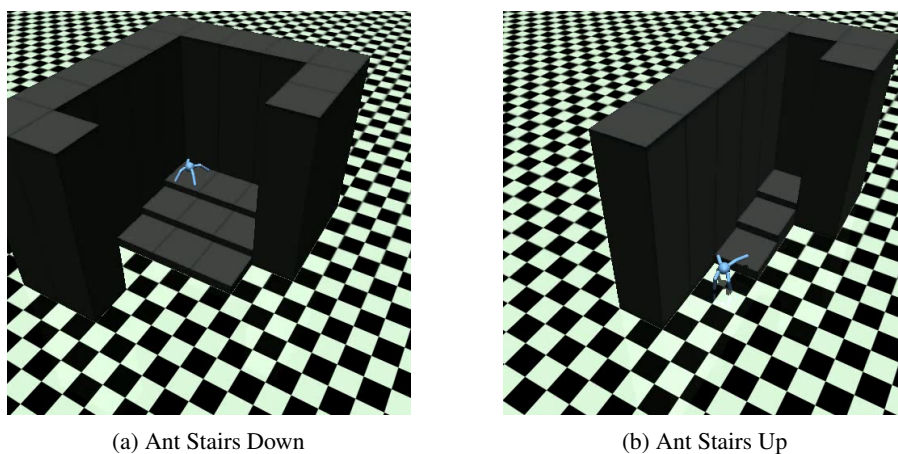


Figure 11: Illustration of the *Ant Stairs* domain. We show a render of the *Ant Stairs Down* environment **(a)** and of the adverse *Ant Stairs Up* environment **(b)**.